Final Report

THE EFFECTS OF SHOCK WAVES ON METEORITES

Prepared for:

HEADQUARTERS
NATIONAL AERONAUTICS AND SPACE ADMINISTRATION
WASHINGTON, D.C. 20546

CONTRACT NASr-49(24)

STANFORD RESEARCH INSTITUTE

MENLO PARK, CALIFORNIA

STANFORD RESEARCH INSTITUTE
MENLO PARK, CALIFORNIA

June 30, 1968

Final Report

THE EFFECTS OF SHOCK WAVES ON METEORITES

Prepared for:

HEADQUARTERS
NATIONAL AERONAUTICS AND SPACE ADMINISTRATION
WASHINGTON, D.C. 20546

CONTRACT NASr-49(24)

By: J. Y. WONG P. S. DE CARLI

SRI Project PGU-6105

Approved: RONALD K. LINDE, CHAIRMAN
Shock and High Pressure Physics Department
Poulter Laboratory

MARJORIE W. EVANS, DIRECTOR
Poulter Laboratory for High Pressure Research

Copy No. 15

CONTENTS

FIGURES

Figures (continued)

TABLES

INTRODUCTION

Shock Effects in Meteorites--General

Meteorites are generally considered to be fragments of one or more parent bodies that formed early in the history of the solar system. Measurements of various isotopic ratios indicate that the oldest meteorites, which include most of the iron-nickel meteorites, solidified about 4.5×10^9 years ago. Studies of nickel diffusion profiles in iron-nickel meteorites indicate that these meteorites cooled from 700° to 300°C at rates which range from $0.4^\circ C/10^6$ years to $40^\circ C/10^6$ years. These cooling rates may be interpreted as indicating that iron meteorites represent portions of cores of differentiated bodies of asteroidal size. Alternatively, one may suggest that the iron-nickel meteorites were at various depths in a mantle of one or more bodies of planetary size. In any case, collisions or explosions, and consequently shock waves, are usually invoked as the explanation for break-up of meteorite parent bodies into the small bodies which eventually fall to the earth as meteorites.

One of the motivations for a detailed study of meteorites is to obtain evidence that may be used to establish and test various models of the formation and history of the solar system. Laboratory study of the effects of shock waves on meteoritic minerals provides the data necessary to differentiate shock effects from primary features which developed within a meteorite parent body. Work on the first part of the present contract was concerned with effects of shock waves on plagioclase feldspars and on selected pyroxene and olivine specimens. The results of the studies performed during the first phase were presented in Quarterly Reports 1, 2, 3, and 4, and in the journal publications listed in Section III of this report.

The present report is concerned with the effects of shock waves on iron-nickel phases in meteorites. Although the experiments performed during the second part of the contract were concerned primarily with iron-nickel meteorites, the results are expected to be applicable to the

the study of stony-iron meteorites and to the study of metal grains in stony meteorites. For the convenience of the reader, this report includes relevant experimental data previously reported in Quarterly Report 5.

Shock Effects in Iron and its Alloys--a Brief History

The study of the effects of shock waves on iron and its alloys can be traced back to French military studies of the mid-nineteenth century. Late in the nineteenth century it was recognized that Neumann lamellae (bands in the microstructure of iron) are formed as a result of shock loading.[1] The relevance of shock wave studies to meteorite research may be indicated by the fact that Neumann lamellae, named after their discoverer, were first recognized in meteorites. These lamellae have been determined to be twin bands, having a $\{112\}$ composition plane and a $< 111 >$ shear direction.[2]

In 1954 Rinehart and Pearson[3] published a detailed account of the mechanical and metallurgical effects of shock waves on metals, in which much new data were presented along with a review of earlier work in the field. They reported a general correlation, in the case of iron, of increasing twin density with increasing shock pressures. They also reported that hardness increases resulting from shock loading were correlated with twin density and that a rather abrupt increase in hardness that was correlated with an equally abrupt microstructural change to a very densely banded structure.

In 1956 Bancroft et al.[4] reported the observation of a double shock wave system which develops in iron shocked to pressures in excess of 130 kbar. They interpreted this double shock system as the result of a dynamic phase change which took place during the passage of the shock at a pressure of approximately 130 kbar. On the basis of a simplified thermodynamic treatment of the effect of pressure on the temperature of the $\alpha \rightarrow \gamma$ phase transition, they suggested that the dynamic transition was probably $\alpha \rightarrow \gamma$. However, subsequent thermodynamic calculations by Curran and De Carli,[5] by Jamieson,[6] and by Kaufman,[7] which differed in detail from one another, all agreed in predicting that pressures in the range 150-170 kbar should be required for the $\alpha \rightarrow \gamma$ transition to occur

at temperatures in the range of 20° to 100°C. In a subsequent metallographic study, Curran et al.[8] reported that the appearance of the heavily banded microstructure in shocked iron was correlated with pressures in excess of 150 kbar. This microstructure, described as "transformation twinned" was attributed to the shock induced $\alpha \rightarrow \gamma$ phase transition which reversed on release of pressure.

In 1962 Fuller and Price[9] reported an abrupt increase in the dynamic electrical resistivity of iron at a shock pressure of 150 kbar. In the same year Johnson et al.[10] suggested, on the basis of metallographic evidence, that the dynamic phase transition was actually to a phase other than α. In their work they assumed that the dynamic phase transition in iron occurs abruptly and is complete at a pressure of 130 kbar. The contradictory evidence presented by Fuller and Price and by Curran et al. was disregarded. Indeed, a careful study of results reported by earlier workers, including Rinehart and Pearson,[3] Tardif et al.,[11] Dieter,[12] and Zukas and Fowler,[13] indicates that the dynamic phase transition is probably smeared out over a 30- to 50-kbar range of pressures.

By 1962 active research on the effect of shock waves on iron and its alloys had virtually ceased. It had become evident that further research, using the techniques then available, was not likely to yield much new information. Although many workers in the field privately expressed reservations concerning the results of Johnson et al., no public controversy arose. Within our own laboratory the decision was made to let the Johnson et al. results stand unchallenged until a restudy of the dynamic behavior of iron could be made with greatly increased precision.

In 1964 Takahashi and Basset,[14] using static high pressure X-ray diffraction techniques, positively identified a close packed hexagonal ϵ phase of iron which is formed near 130 kbar and which is not retained on relase of pressure to 1 atmosphere. Since that time most workers in the high pressure field have assumed that the phase transition inferred from shock wave studies is identical with the statically observed $\alpha \rightarrow \epsilon$ transformation and that the shock wave transition occurs abruptly

at a pressure of 130 kbar. It has also been assumed that the equilibrium pressure-temperature (P,T) phase diagram of iron was accurately determined in the shock compression study of Johnson et al., and this phase diagram has been used to obtain calibration points for static high pressure studies.

During the past few years there has been a revival of interest in the effects of shock waves on metals, with particular emphasis on the effects of shock waves on meteoritic irons. In order to adequately interpret the changes in microstructure and mechanical properties that result from the shock loading of meteoritic nickel-iron alloys, it is necessary to consider the possibility of shock-induced phase transitions. The metallographic changes observed in the kamacite phase of shocked meteorites are similar to the changes observed in shocked iron and low carbon steels. It is generally assumed that kamacite, like pure iron, transforms during shock compression to a close packed hexagonal ϵ phase. The heavily banded kamacite microstructure observable in some "as found" meteorites (e.g., Grant) and in meteorites which have been subjected to laboratory shocks to pressures of 200 kbar or higher, is variously referred to as the "ϵ structure," the "ϵ transformation structure," or the "matte structure." Unfortunately, current knowledge of the behavior of iron-nickel alloys under shock loading depends heavily on the validity of the Johnson et al. study of iron as well as on the currently fashionable view that the dynamically inferred and statically observed high pressure transformations of iron are identical.

The validity of the assumption used in the Johnson et al. work that the boundary separating zones of different microstructural changes corresponded to the line at which the pressure in the second shock wave of the double shock system dropped to the phase transition pressure, 130 kbar at 300°K, was finally challenged in the open literature late in 1965 by the work of Nivikov et al.[15,16] These authors argued that the position of the zone boundary corresponds to a level of pressure in the second wave higher than the phase transition pressure. They attempted to repeat the Johnson et al. work by studying the dynamic (α , ϵ) phase line of Armco iron using the "capacitor" method for detecting the two-wave

system that forms in iron above the phase transition pressure. However, their data show considerable scatter and do not appear to correlate with the results of previous workers. We have serious doubts about the accuracy of their experimental method and we take exception to their view that the dynamically inferred and statically determined (P, T) phase diagrams of iron should be identical.

At the start of the present program it was becoming generally evident to high pressure researchers that further work on the shock wave induced phase transition in iron was needed. The discrepancies among shock wave transition pressures reported by different workers were too large to be ignored. It also became clear that substantial progress could be made not by repeating the pioneering experiments on the iron transition, but rather only by taking advantage of new techniques of shock wave measurement.

SUMMARY

The primary objective of the study was to analyze the effects of shock waves on the metallic minerals in meteorites, namely iron and iron-nickel alloys. The study was divided into two parts: Part I was concerned with the investigation of temperature pressure dynamic phase diagrams. Part II was devoted to the study of residual effects caused by the shock loading of iron and iron-nickel alloys, emphasizing experiments on selected meteoritic material.

The first portion of Part I concentrated primarily on the testing of a new experimental method for determining the $\alpha \rightarrow \epsilon$ transition pressure of iron, which could lead to high accuracy, combined with a substantial saving of time and effort in determining the dynamic (P, T) phase diagram of iron and iron-nickel alloys. During the testing of this method it was discovered that ϵ-iron, once formed, does not automatically revert to α-iron upon pressure release (experimental pressure release was 36 kbar/μsec beyond the time of passing through the $\alpha \leftrightarrow \epsilon$ transition pressure). Although this highly significant discovery does not rule out completely the workability of the new method, it appears that a more conventional resistivity technique is a better method for studying dynamic temperature-pressure phase diagrams of iron and iron-nickel alloys.

The second portion of Part I was devoted to a careful reinvestigation of the dynamic response of α-iron to shock loading using an improved technique for measurement of electrical resistivity during shock compression. This investigation yielded data that are in substantial disagreement with the phase transition results obtained by Fuller and Price. However, the present data are consistent with the static data of Balchan and Drickamer. Moreover, the present dynamic data resolve for the first time the discrepancy between the observation of three stable shocks in iron starting at 130 kbar by Bancroft et al. and the evidence by two recent investigations by Curran and by Katz et al. that the shock pressure required to produce the metallographic "matte" appearance associated with the 130-kbar dynamic transition may be $\sim$ 155 kbar. A

critical comparison between the present techniques and those used by Fuller and Price led to the conclusion that the present data are more reliable. It is believed that the present investigation has significantly increased the level of understanding of the dynamic transition of α-iron to high pressure phases.

A resistance heating technique for varying the initial temperature of iron or iron-nickel alloy specimens used as piezoresistive elements in resistivity techniques for studying polymorphic transitions has been successfully developed in this project. This development includes the calibration between the temperature and the amplitude and duration of the heating current for iron.

Another technique developed during this project utilizes the shock-induced transient demagnetization eddy current spike for monitoring the completeness of polymorphic transitions involving a magnetic phase. This new technique furnishes a very useful supplementary tool to the conventional resistivity techniques in the studies of phase transitions of iron and iron-nickel alloys.

Part II of this program was concerned with the study of permanent shock-induced damage in meteorites. Samples of iron-2.5% silicon single crystals, the Karee Kloof coarse octahedrite, and the Hoba ataxite were shocked to pressures ranging from 35 kbar to 480 kbar. For 35-, 70-, and 90-kbar experiments, the major effect of shock waves on the iron-2.5% silicon and Karee Kloof kamacite was twinning. The density of shock induced twins increased with increasing pressure. The 235- and 480-kbar specimens of iron-silicon and Karee Kloof kamacite showed the "matte" microstructure, which is generally considered to be evidence of a shock induced phase transformation. Specimens of shock loaded Hoba were only marginally distinguishable from control specimens. Hardness and annealing studies were also performed on the shocked samples.

I. PHASE DIAGRAMS

A. Introduction and Background

The pressure-temperature phase diagram of iron has been investigated by static high pressure techniques and by dynamic high pressure (shock wave compression) techniques. Static high pressure measurements of iron phase equilibria have been conducted in a pressure-temperature region in which pressure calibrations are highly uncertain. Consequently, available dynamic (shock wave) data have been used to obtain calibration points for static high pressure apparatus. The implicit working hypothesis has been that dynamic phase transitions occur at pressure-temperature equilibrium points. This hypothesis has not yet been proven for any material, and it has been false in many cases.[17]

A phase transition can be detected by dynamic measurement techniques only if a finite portion of the material under observation transforms during the few microseconds available for observation. To provide sufficient driving force for this partial transformation to occur in such limited time, a pressure in excess of equilibrium may be required. Most shock wave measurements have one-dimensional shock propagation geometries; the material under investigation is therefore subjected to plane strain as opposed to hydrostatic strain in ideal static high pressure experiments. For a material with finite yield stress under shock compression, the dynamic compression curve (Hugoniot) will exceed the hydrostatic value at a given strain by two-thirds the yield stress. One might therefore expect a similar offset in dynamic phase transition pressures relative to equilibrium pressures. On the other hand, some phase transitions may be kinetically aided by non-hydrostatic strain or by the high strain rates available in shock compression experiments. It would appear that relationships between dynamically determined phase transitions and equilibrium phase boundaries must be determined empirically for individual materials. From considerations of phase transformation kinetics, the transition pressure determined by shock wave techniques should in most cases be an upper bound on the equilibrium (static) transition pressure.

Since the shock history of fallen meteorites is dynamic, rather than static, the dynamic pressure-temperature phase diagrams of meteoritic materials are the appropriate ones to use in the study of shock effects on meteorites.

It is generally believed, that the most accurate equilibrium ("static") pressure-temperature (P,T) phase diagram of iron is that obtained by Bundy,[18] using static high temperature and high pressure resistivity techniques. He calibrated his apparatus with respect to the triple point (α, γ, ϵ) of iron at 110 kbar and 500°C obtained by Johnson et al.[10] in their shock compression experiments. In the latter work it was possible that some recrystallization in the recovered specimens may have occurred that was unrelated to the different microstructures achieved upon shocking initially α-iron into the pressure-temperature field on both sides of the triple point (driving the material into the ϵ-phase below 500°C and into the γ-phase above 500°C). Hence the location of the triple point (α, γ, ϵ) of iron at 110 kbar and 500°C in the (P,T) phase diagram as reported by Johnson et al.[10] might not be accurate. Although Bundy's phase diagram of iron includes the 130-kbar and 37°C $\alpha \rightarrow \epsilon$ transition point established by Bancroft et al[4] and by Perez-Albuerne et al.,[19] it is in marked disagreement with the dynamic high pressure resistivity data of Fuller and Price,[9] who placed the $\alpha \rightarrow \epsilon$ polymorphic transition of iron at 150 kbar and $\sim$ 100°C.* In view of the discrepancy in transition pressures it is important to reinvestigate the dynamic high temperature and high pressure phase diagram of iron using more precise techniques of measurement than were available to Johnson et al.[10]

It has been reported[18,20] that the resistivities of α-, ϵ-, and γ-iron have roughly the ratio of 1:2:5 at room temperature and atmospheric pressure and that they possess large temperature coefficients but relatively small pressure coefficients. Thus, as explained below,

---

* Bancroft et al.[4] and Fuller and Price[9] actually associated the dynamic transition they observed with the static $\alpha \rightarrow \gamma$ transition of iron. However, most workers in the field[6,14] currently identify the observed dynamic transition with the static $\alpha \rightarrow \epsilon$ transition of iron.

by using a thin iron wire as a piezoresistive element (similar to the manganin* pressure transducer),[21] it is possible to determine the pressures associated with polymorphic transitions of iron by measuring the resistivity of the wire as a function of pressure and detecting the abrupt changes in resistivity which occur at phase transitions (see Fig. 1).

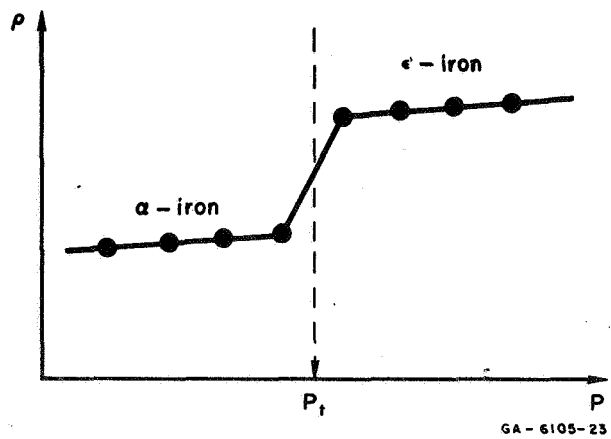

FIG. 1 PIEZORESISTIVE BEHAVIOR OF IRON IN THE PHASE TRANSITION REGION
P_t = Transition Pressure

The ratio of the resistivities of the transformed and original phases may not be the same as that determined statically, since the presence of shock induced defects may change the resistivity of both phases. Furthermore, a discontinuity in resistivity would also result from a partial transformation, and the resistivity ratio would depend on the completeness of the transformation. Fuller and Price[9] reported that the ratio of the dynamic resistivities of the transformed and original phases agreed fairly well with that determined statically in the pressure range from 0 to 350 kbar. They also reported that the resistivity of α-iron does not vary appreciably with pressure from 0 to 150 kbar. Thus their results imply that the resistivities were

*Manganin is an alloy with nominal composition of 84% Cu, 12% Mn, and 4% Ni.

not altered appreciably by the presence of shock induced defects and that the bulk of α-iron had undergone transformation to the new phase when shocked to pressures only slightly above the transition pressure.

To estimate the temperature of the iron wire at the phase transition, it is necessary to correct for the generation of heat by shock compression. Because the resistivity of iron depends on pressure and temperature, among other factors, an independent measurement must be employed to obtain the pressure in the iron specimen. Using a manganin gage for pressure calibration, Fuller and Price[9] reported a transition in α-iron at 150 kbar and ~ 100°C.

The configuration and dimensions of the iron specimen used in the present piezoresistivity studies are shown in Fig. 2. (The installation of iron specimens in targets is described in detail in Section B-2-a, below.) The iron wire used is 99.99% pure and 0.003" in diameter. The

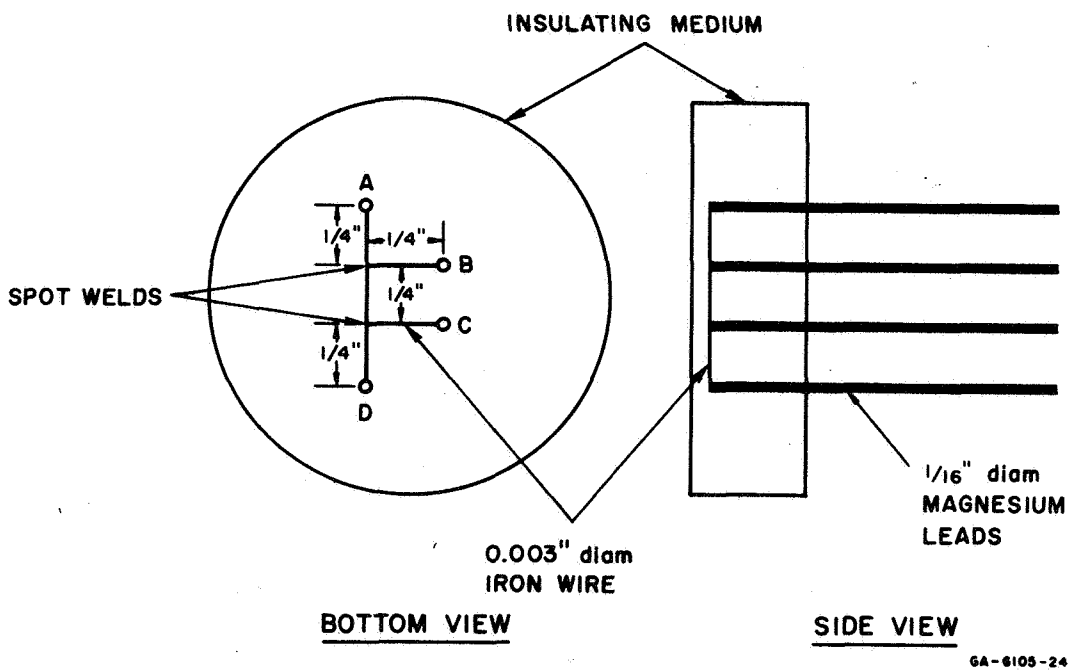

FIG. 2 IRON WIRE USED AS PIEZORESISTIVE ELEMENT IN INSULATING MEDIUM

piezoresistive element has four poles,* A, B, C, and D, soldered to four 1/16" diameter magnesium leads and is imbedded in an insulating medium. During the shock experiment a constant current pulse is applied across the outer terminals A and D, and the resistivity of the iron specimen is monitored by measuring the voltage across the inner terminals B and C. Thus, by applying shocks of different magnitudes to the specimen, the resistivity of the iron specimen as a function of pressure can be obtained.

The initial temperature of the iron specimen may be varied by preliminary resistance heating. By varying the amplitude and duration of the heating current, the initial temperature of the iron specimen can be set at any temperature up to its melting point. The temperature can be calibrated with respect to the amplitude and duration of the heating current by measuring at atmospheric pressure the resistivity of the specimen at various temperatures (as determined by a thermocouple) and observing the amplitude and duration of the heating current needed to reproduce the same values of resistivity at these temperatures (see Section B-2-c).

Thus, by starting with α-iron wire used as a piezoresistive element imbedded in an appropriate insulator such as Lucalox† ceramic and varying its initial temperature, the (α, ϵ) and (α, γ) phase lines of the dynamic (P,T) phase diagram of iron can be obtained. Only the temperature rise due to shock heating must be estimated independently. This rise is small, however, since the pressures involved are not very high ($<$ 150 kbar). For example, the temperature rise due to shock heating for iron singly shocked to 130 kbar has been estimated to be

---

* Fuller and Price[9] used a two-pole configuration in their experiment. With the two-pole configuration the accuracy of measurements can be greatly affected by contact resistance. With the four-pole configuration, as used in the present experiments, the uncertainty in resistance due to contact resistance is negligible.

† A General Electric Company brand name for polycrystalline alumina (ρ = 3.98 g/cm^3),[22] which has a shock impedance close to that of iron in the pressure range 0 to 500 kbar.

less than 40°C.[4,23] The shock temperatures along the iron Hugoniot can be estimated with fair accuracy up to about 130 kbar, using existing calculation methods.[23,24]

Obtaining the (γ, ϵ) phase line of the dynamic (P,T) phase diagram of iron is much more difficult because of the small difference in resistivity between γ- and ϵ-iron at temperatures of 500°C and above and because one has to start with γ-iron, which is stable only at high temperatures (> 900°C at atmospheric pressure) or high pressures (~ 110 kbar at 500°C).[18] However, it is possible to obtain this phase line with a double shock experiment. In such an experiment the α-iron is first heated to 500°C (or above) and is then subjected to two consecutive shocks designed so that the first one sends the iron into the γ-field at a temperature only slightly above its initial temperature and the second shock reinforces the first shock and sends the iron into the ϵ-field. The abrupt change in resistivity which results from the phase change caused by the second shock can then be detected.

The second shock can be most easily obtained by reflecting the first shock off a material with a higher shock impedance than the insulating medium in which the iron specimen is imbedded. The magnitude of the first shock must be of sufficient strength to send the α-iron specimen into the γ-field. The amplitude of the reflected shock can be varied by changing the amplitude of the first shock.

Any of the above techniques can be employed to obtain the (α, ϵ), (α, γ), and (γ, ϵ) dynamic (P,T) phase lines for the various iron-nickel alloys. These techniques are time consuming, however, and hence rather costly for phase boundary studies. Because only one resistivity pressure point per shock experiment can be obtained by such methods, one generally must perform on the order of six or more shock experiments to accurately establish the pressure at which the jump in resistivity occurs, and thus determine one point in the (P,T) phase diagram.

For this reason the first portion of the project effort was devoted largely to the development of a more efficient experimental method. The method that was devised takes advantage of the fact that shock waves

generated by thick high explosive pads have profiles similar to the one shown in Fig. 3 (a) instead of that in Fig. 3 (b). After the peak pressure P_o has been reached, the pressure is attenuated by a rarefaction wave originating from the expanding gases of the explosive behind the initial shock and moving more rapidly than the shock. We then have a means of varying pressure continuously from P_o to pressure P in time t_o [see Fig. 3 (a)]. Both P_o and t_o can be varied: P_o by choosing an appropriate explosive system, and t_o by building a target of proper geometric design to keep any unwanted rarefactions away from the specimen for a sufficiently long time. If P_o is adjusted to be greater than the polymorphic transition pressure P_t, and t_o is designed to be long enough so that the pressure decreases to $P < P_t$ before spurious rarefactions reach the specimen, then the abrupt change of resistivity accompanying the inverse transition, from ϵ to α, for example, can be located, and hence the value of P_t can be determined in a single shock experiment (see Fig. 4). A manganin pressure gage can be used to monitor the pressure of the iron specimen. From considerations of phase transformation kinetics, the transition pressure associated with the dynamic inverse transition should be a lower bound on the equilibrium (static) transition pressure.

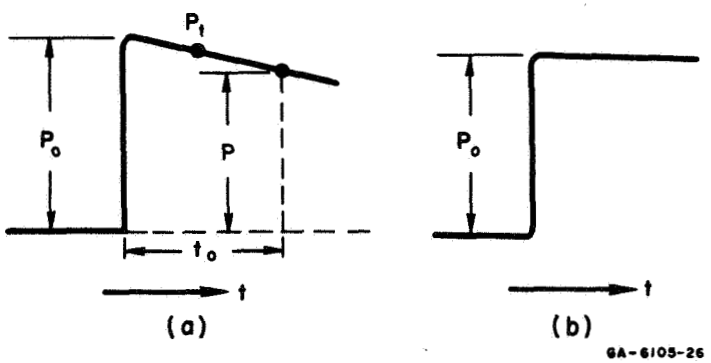

FIG. 3 SHOCK WAVE PROFILES (a) WITH ATTENUATION AND (b) WITHOUT ATTENUATION

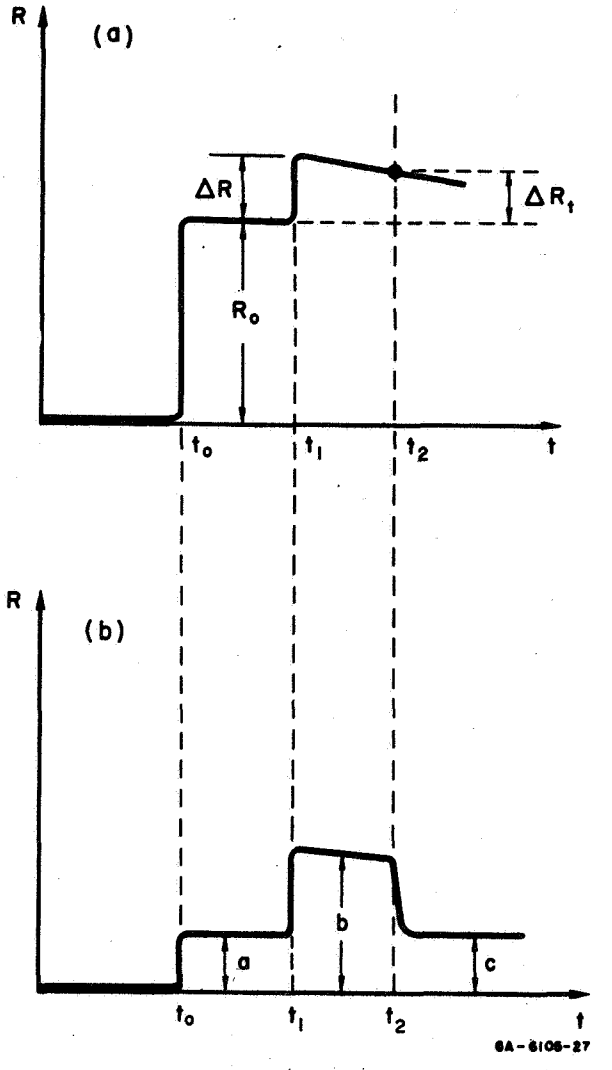

FIG. 4 DETERMINATION OF $\epsilon \rightarrow \alpha$ TRANSITION PRESSURE OF IRON; (a) MANGANIN GAGE RECORD, (b) IRON SPECIMEN RECORD

Figs. 4 (a) and 4 (b) show schematically the manganin transducer and iron specimen records, respectively. At $t = t_o$ the "viewing" current is turned on; the atmospheric pressure resistances of the manganin gage and iron specimens are given by R_o and a, respectively. At $t = t_1$ the shock arrives, and its peak pressure is given by the ratio $\Delta R/R_o$ of the manganin gage (corresponding to $P_o > P_t$). The resistance step b in the iron record represents the resistance of the

ϵ-iron at pressure P_o. At $t = t_2$ the pressure experienced by the iron specimen has decreased to P_t (corresponding to $\Delta R_t/R_o$ of the manganin gage record) and there is an abrupt change of resistance (b $\rightarrow$ c) in the iron record. Thus, by locating the position of this abrupt change, P_t can be obtained directly from the manganin gage record. (We have implicitly assumed that the transition $\alpha \longleftrightarrow \epsilon$ is reversible within a very short time. This has been implied indirectly by Erkman.)[25]

When a magnetic and a nonmagnetic phase are involved in a polymorphic transition, as in the case of the α- (magnetic) and ϵ- (nonmagnetic) iron, there is another method of monitoring the phase transition as a function of pressure. When the specimen is used as a piezoresistive element the "viewing" current sets up a large magnetic flux in the specimen when the specimen is magnetic in the initial phase. During the transition to a nonmagnetic phase the magnetic permeability changes from a large value ($\sim 10^3$ for iron) to ~ 1 in a very short time, and the material in the new phase can no longer support such a large magnetic flux. The repulsion of the flux from the specimen induces a transient eddy current, which appears as a spike in the resistivity record of the specimen. The observation of such an eddy current spike associated with the $\alpha \rightarrow \epsilon$ transition of iron has recently been reported.[26] In this reported work the iron specimen was in the form of a thin strip and the geometry was therefore one-dimensional. In the present work the iron specimen took the form of a thin wire (three-dimensional geometry) and a similar transient was observed (see Fig. 5). If the peak pressure exceeds the transition pressure, and the pressure is allowed to decrease undisturbed to less than P_t, then there will be two such eddy current transients--one associated with the $\alpha \rightarrow \epsilon$ and the other with the inverse $\epsilon \rightarrow \alpha$ transition. By detecting the location of the second transient in the iron record, one can obtain P_t from the accompanying manganin transducer trace (Fig. 6). In the figure the $\epsilon \rightarrow \alpha$ transition takes place at $t = t_2$, as indicated by the eddy current transient, and P_t corresponds to $\Delta R_t/R_o$ of the manganin record.

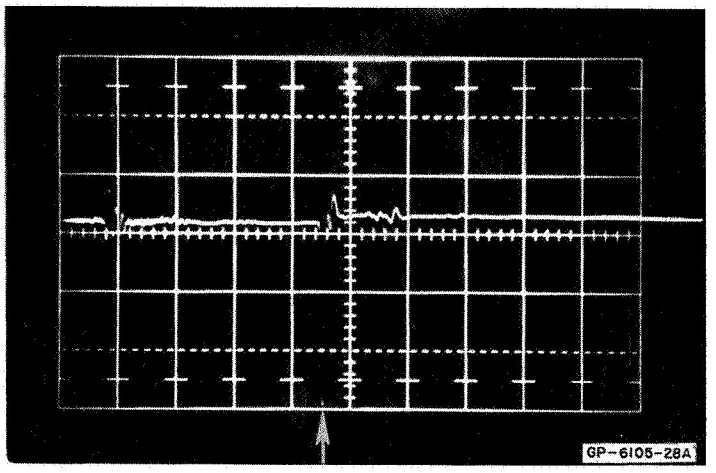

FIG. 5 EDDY CURRENT TRANSIENT ASSOCIATED WITH $\alpha \rightarrow \epsilon$ POLYMORPHIC TRANSITION OF IRON. Horizontal scale = 0.2 μsec/cm; initial peak pressure in iron specimen = 190 kbar.

When a fully or partially magnetized magnetic material is subjected to a shock the material will be temporarily or permanently demagnetized. The resultant change of magnetization of the material sets up a transient eddy current, which can be detected electrically as a voltage spike. There are at least three possible mechanisms for demagnetization of a magnetic material by a shock.[27] The first one is shock induced phase change, as in the case of iron which has been discussed previously. The second one is shock induced misalignment of magnetic domains dues to strain rate effects or local microscopic strain. The third one is shock induced magnetic anisotropy arising from the anisotropic microscopic strain associated with the shock. When α-(magnetic) iron is used as a piezoresistive element as discussed above, the "viewing" current sets up a large magnetic field in the material (in this case the iron wire) and the latter is almost completely magnetized. For a typical "viewing" current of ~ 3 amp the magnetic field set up in an iron wire of 0.003" diameter varies linearly from zero oersted at the center of the wire to ~ 300 oersteds at its surface. Since the coersive force of iron is ~ 1 oersted, and there is no demagnetization field in the case of a current flowing in a wire, the wire will be completely magnetized except for very small regions near the center and along the axis of the wire

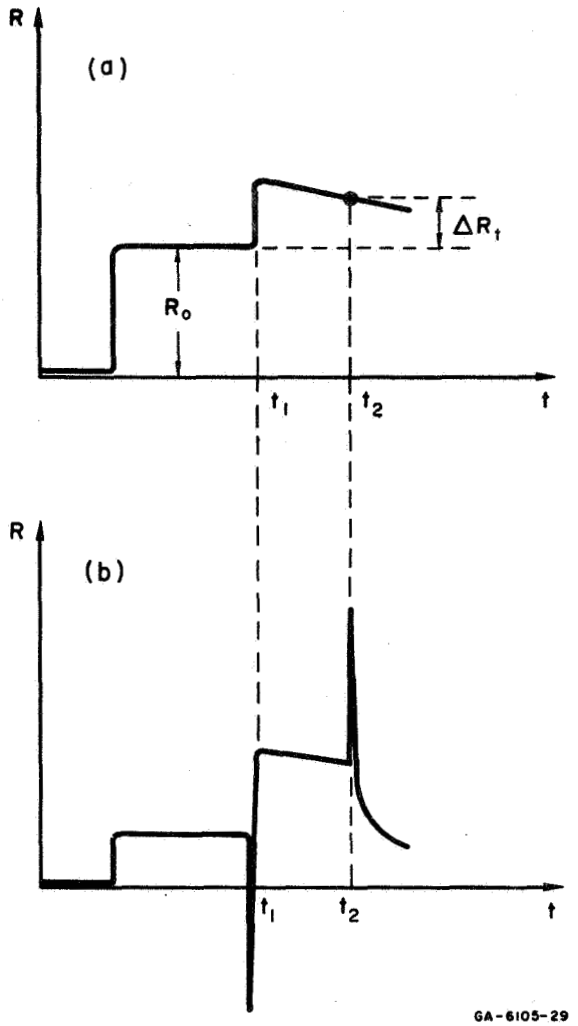

FIG. 6 DETERMINATION OF $\epsilon \rightarrow \alpha$ POLYMORPHIC TRANSITION PRESSURE OF IRON USING EDDY CURRENT TRANSIENTS; (a) MANGANIN GAGE RECORD, (b) IRON SPECIMEN RECORD

where the magnetic field set up by the "viewing" current is less than 1 oersted. When the specimen is subjected to a shock, demagnetization eddy currents will be induced in the specimen similar to those accompanying the $\alpha \rightarrow \epsilon$ polymorphic transformation even though the magnitude of the shock is well below that corresponding to the transition pressure. This demagnetization is probably caused by shock induced misalignment of magnetic domains or shock induced magnetic anisotropy. Such transient eddy current spike has been detected in the present work and is shown

in Fig. 7. This demagnetization eddy current spike can be used to obtain the pressure at which α-iron is completely transformed into ϵ-iron. This is done with a double shock experiment. A shock of variable magnitude is sent into the specimen, followed by a second weaker shock. So as long as the magnitude of the first shock is not large enough to cause a complete transformation of α-iron into ϵ-iron, two eddy current spikes will be observed. However, when the magnitude of first shock is large enough to do so only one eddy current spike caused by the first shock will appear. The second weaker shock will not cause any demagnetization eddy current spike since the ϵ-iron is nonmagnetic.

B. Experimental Studies

1. Outline

The first portion of this part of the project was devoted mainly to the testing of a more efficient method for determining the $\alpha \rightarrow \epsilon$ transition pressure of iron, as discussed in Section A. Such a method could eventually lead to a substantial saving of time and effort in determining the (P,T) phase diagrams of iron and iron-nickel alloys.

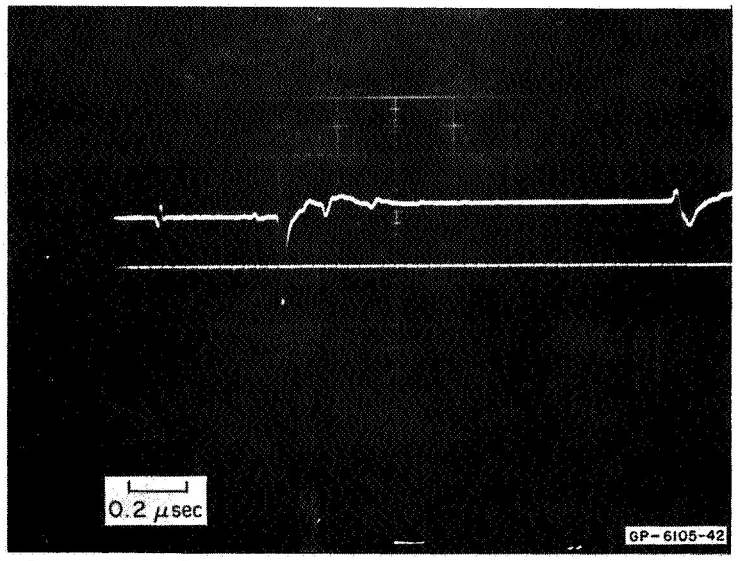

FIG. 7 EDDY CURRENT TRANSIENT ASSOCIATED WITH SHOCK DEMAGNETIZATION IN IRON AT 45 kbar

The remaining portion of this part of the project was concentrated on: (1) a careful reinvestigation of the response of α-iron to shock loading with an improved resistivity technique based on the same principle used by Fuller and Price;[9] (2) the development of a method of varying the initial temperature of iron or iron-nickel alloy specimens used as piezoresistive elements in resistivity techniques for determining polymorphic transition pressures of these materials; and (3) the determination of the pressure (at one particular temperature) above which the $\alpha \rightarrow \epsilon$ transformation of iron is complete by designing double shock experiments and utilizing the shock induced transient demagnetization eddy current spike.

2. Experimental Methods

a. Testing of New Experimental Method

A total of five shock experiments (Shot Nos. 13,252-53, 13,317-18, and 13,330) were performed in order: (1) to generate an adequate decreasing pressure ramp extending from $\sim$ 190 kbar to $\sim$ 100 kbar in $\sim$ 2 μsec; and (2) to determine the $\alpha \rightarrow \epsilon$ transition pressure of iron by detecting the transient eddy current spike associated with the $\epsilon \rightarrow \alpha$ polymorphic transformation of iron.

The explosive system employed in these five shock experiments is shown in Fig. 8. The specific plane wave generator, explosives, and driver plate materials used in each individual shock experiment are summarized in Table I (see Section B-3-a). Preliminary experiments cited in Progress Report No. 5 showed that the use of C-7 epoxy as insulating material in the construction of targets leads to very high shock temperatures in the iron specimen caused by impedance mismatch. Hence, Lucalox ceramic, which has a shock impedance close to that of iron in the pressure range 0 to 500 kbar, was used as the insulating material in the construction of all subsequent targets.

Since the release adiabats of the explosives used were not known well enough to permit an accurate determination of shock pressures by the impedance match method, all targets for these five shock experiments consisted of a manganin gage for indicating the pressure, in addition to

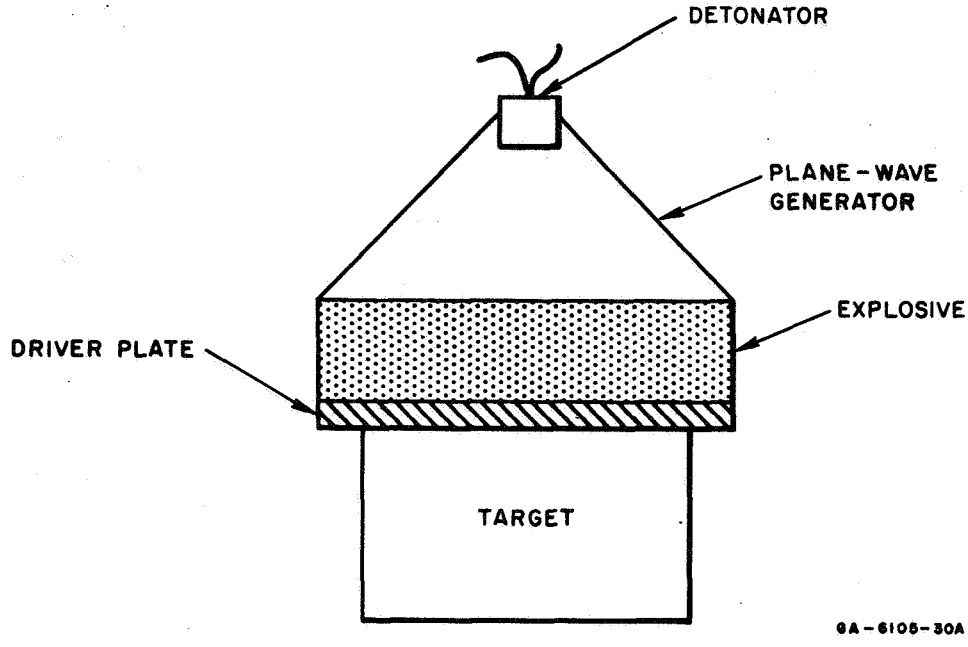

FIG. 8 EXPLOSIVE ASSEMBLY

an iron gage installed in Lucalox ceramic. The detailed construction of one of these targets is shown in Fig. 9. Two sets of four 3/32" diameter holes were drilled in a 2" diameter by 1" thick Lucalox disc with one face ground flat (Fig. 9). The iron or manganin gage element (see Fig. 2) was flattened to $\sim$ 0.0015" and laid on the ground face of the Lucalox disc with its four terminals bent back through the holes in the Lucalox. The gage element was maintained flat on the ground face of the Lucalox disc by cementing a Lucalox backing plate ($\sim$ 0.035" thick and ground flat and parallel on both sides) to it with C-7 epoxy, as shown in Fig. 9. The holes were stuffed with amalgam approximately halfway up from the bottom to insure good electrical contact with the gage terminals, and brass leads (1/16" diameter) were then inserted into the holes and secured in position with conductive epoxy. Another layer of Epon (R) epoxy* was applied on top of the conductive epoxy to strengthen the joints between the brass leads and the gage terminals.

* A brand name of epoxy manufactured by Shell Chemical Company, Pittsburg, California.

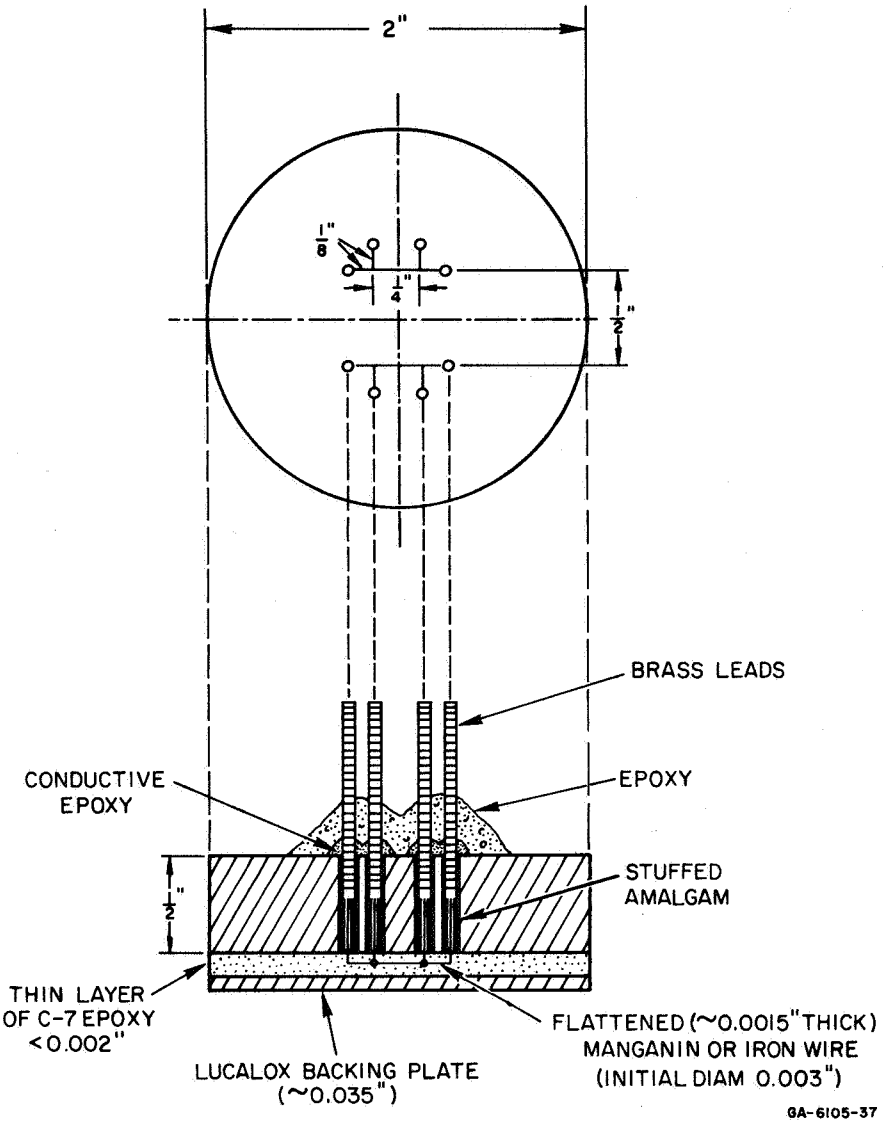

FIG. 9 TARGET CONSTRUCTION SHOWING DETAILED INSTALLATION OF PIEZORESISTIVE ELEMENTS IN LUCALOX CERAMIC

Since the method we employed to install the manganin gage in our targets (see Fig. 9) is quite different from that commonly used, in which the gages are installed entirely in C-7 epoxy, a new pressure calibration of the manganin gages was necessary. This was done in the series of gun shots described in the next section (see Section B-2-b).

b. $\alpha \rightarrow \epsilon$ Transition of Iron

Eight shock experiments (Shot Nos. 13,477-13,484) were performed using the SRI gas gun in order to reinvestigate the dynamic $\alpha \rightarrow \epsilon$ transition of iron using an improved resistivity technique based on the same principle used by Fuller and Price (see Section A). The gas

gun was used instead of explosives for more freedom in varying the pressure of the shots. With the exception of Shot No. 13,482, whose target consisted of one manganin and one iron gage, all the targets of the other shots had one nickel gage in addition. Since nickel is known to have no polymorphic transitions in the pressure range 0 to 500 kbar, the nickel gage was used as a control. Lucalox ceramic was used as the insulating material in all these targets, and the procedures for the construction of these targets were exactly the same as those described previously (see Fig. 9).

Since the velocity of a projectile in a gun shot can be measured accurately, the shock pressure in the target may be obtained by the impedance match method provided that the Hugoniots of the target and projectile materials are available. In this case the Hugoniots of the projectiles (aluminum and brass) and target materials (Lucalox ceramic) are well-known, which permitted the pressure calibration of the manganin gage installed in Lucalox ceramic in the present series of gun shots. As pointed out in Section B-2-a, above, this calibration is necessary in order to determine the shock pressures obtained in the previous explosive shots.

c. Temperature Calibration

It was pointed out in Section A that one of the advantages of using the resistivity technique in the determination of the dynamic high pressure and high temperature phase diagrams of iron and iron-nickel alloys is the ease of varying the initial temperature of these materials by preliminary resistance heating. In order to achieve this, the calibration between the temperature of these materials and the amplitude and duration of the heating current must be known. For iron and iron-nickel alloys, which have large temperature coefficients of resistivity at atmospheric pressure, the temperature of these materials can be obtained from their resistivity if the latter is known as a function of temperature. If, in addition, the resistivity of these materials is calibrated with respect to the amplitude and duration of the heating current, we have in effect a calibration between the temperature of these materials and the amplitude and duration of the heating current.

The relative resistance (with respect to room temperature) of iron at atmospheric pressure as a function of temperature was obtained by: (1) installing the iron specimen as a four-terminal piezoresistive transducer (see Fig. 2) between two Lucalox ceramic discs, which were

bolted toegher with tantalum threaded rods and nuts and wound with ~ 20 ft of 0.010" diameter manganin heating wire (3 Ω/ft), as shown in Fig. 10; (2) varying the temperature of the iron specimen by varying the temperature of the Lucalox ceramic discs via resistance heating; and (3) monitoring the resistance of the iron specimen as its temperature was being varied by applying a constant current pulse across its outer terminals and measuring the voltage across its inner terminals (see Fig. 2). The temperature of the Lucalox ceramic, and hence that of the iron specimen, was monitored with a chromel-constantan thermocouple.

A constant high current power supply (35 amp at 3.5 Kv) with a variable output duration control has been designed and constructed for use in the resistance heating of the iron specimen employed as piezo-resistive transducers. The circuit diagram of this unit is shown in Fig. 11.

d. Pressure Necessary for Complete Transformation of α- to ϵ-iron

Four double shock experiments (Nos. 13,345, 13,330, 13,253 and 13,252) utilizing the shock induced transient demagnetization eddy current spike as discussed in Section A above were performed in order to determine the pressure above which the $\alpha \rightarrow \epsilon$ transformation of iron is complete. Except for shock heating the iron specimen was initially at room temperature. With the exception of Shot No. 13,345, the shots have been described before (see Table I). The targets of these four shots all contained one manganin and one iron gage installed in Lucalox ceramic. The construction of these targets has been described previously (see Fig. 9). In these four experiments the main shock was always followed by a second weaker shock approximately 0.2 μsec after the arrival of the main shock. (In some cases there were two or more such weaker shocks equally spaced with respect to the main shock (see Fig. 7).) This weak second shock is due to the reflection of the main shock off the thin layer of C-7 epoxy separating the Lucalox backing plate and the gage elements (see Fig. 9). Since Lucalox has a higher shock impedance than the C-7 epoxy, this reflection is a rarefaction wave. After traversing the thickness of the Lucalox backing plate, this rarefaction wave is

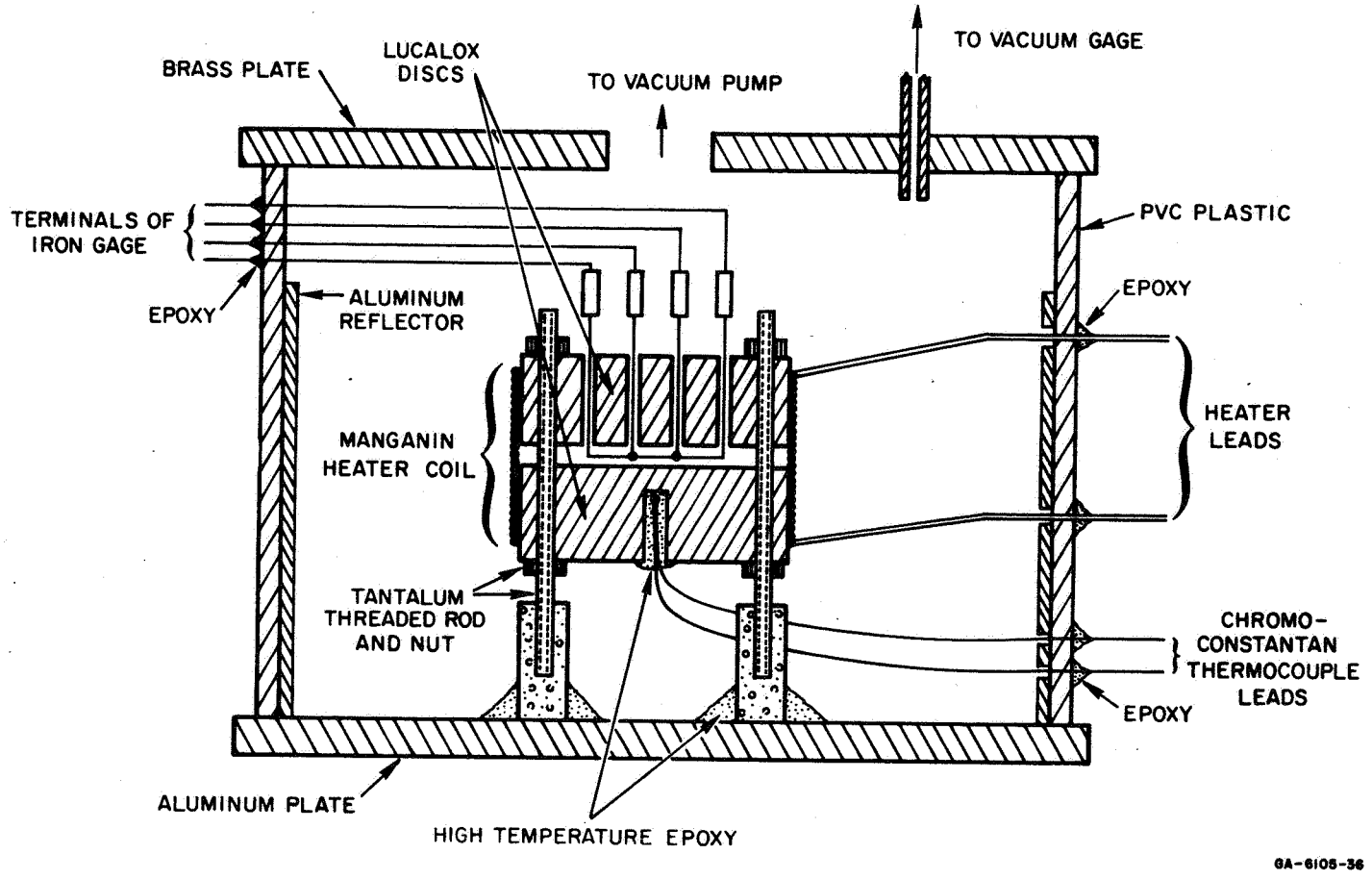

FIG. 10 HEATING ASSEMBLY FOR OBTAINING RELATIVE RESISTANCE OF IRON AS A FUNCTION OF TEMPERATURE

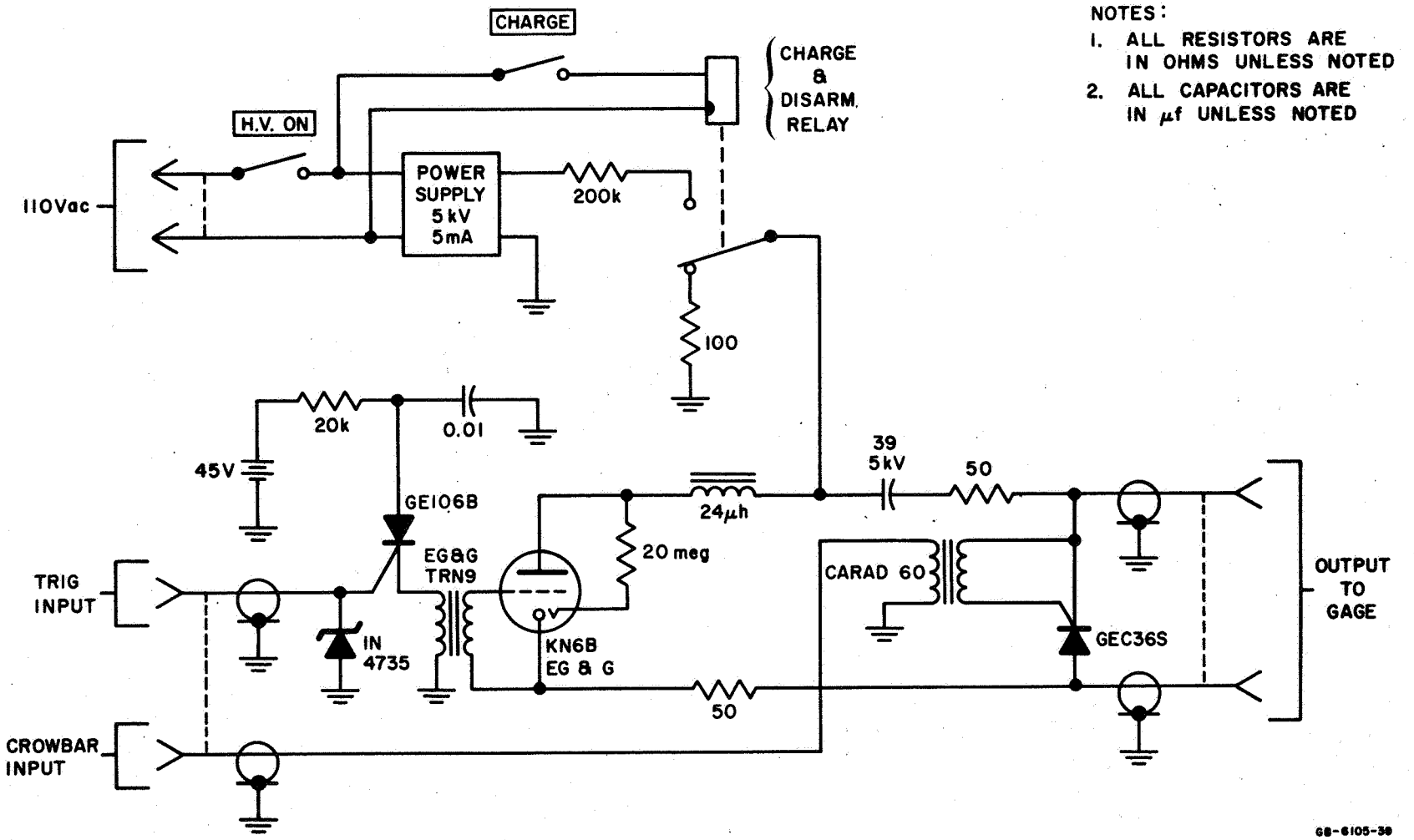

FIG. 11 CIRCUIT DIAGRAM OF HIGH CURRENT POWER SUPPLY

reflected off the explosive gases, which have a lower shock impedance than the Lucalox ceramic, and a compressional wave travels back in the same direction as the original shock, thus giving rise to the second weaker shock. Shot No. 13,345 was designed to confirm the origin of this second weaker shock by doubling the thickness of the Lucalox backing plate so that the separation in time between the second shock and the main shock should be roughly twice that of the other shots.

3. Experimental Results

a. Testing of New Experimental Method

The results of the five shock experiments are summarized in Table I. Despite the fact that an adequate decreasing pressure ramp of ~ 2 μsec duration has been successfully generated (Shot No. 13,317, Table I), no transient eddy current spike associated with the $\epsilon \rightarrow \alpha$ polymorphic transition was observed. Fig. 12 (a) shows the decreasing pressure ramp extending from 184 kbar to 112 kbar. Fig. 12 (b) shows the iron resistivity record. The demagnetization eddy current spikes caused by shock induced phase change ($\alpha \rightarrow \epsilon$) can be seen at the beginning of the record (see Fig. 12 (b)). The double spike results from the fact that for pressure above the Hugoniot elastic limit of Lucalox ($\sim$ 120 kbar) two waves were formed in Lucalox with the elastic wave traveling faster than the plastic wave by ~ 2 mm/μsec.[10] Since the shock had to traverse the Lucalox backing plate, by the time this shock reached the gage elements it separated into two shocks, thus causing the feature of the double spike in the iron resistivity record. It can be seen from Fig. 12 (b) that no more eddy current spike appears after the first double spike even though the initial and final pressures of the pressure ramp are well above and below, respectively, the currently believed transition pressure ($\sim$ 130 kbar).

b. $\alpha \rightarrow \epsilon$ Transition of Iron

The results of the eight shock experiments are summarized in Table II. Some pertinent results obtained in the previous five explosive shots (Shot Nos. 13,252-53, 13,317-18, 13,330) are also incorporated in this table. The resistivity data for both iron and nickel are plotted in Fig. 13. The resistivity data of Fuller and Price for iron[9] are also included in this figure.

TABLE I

Results of Pressure Ramp Experiments

Shot No.	Plane-Wave Generator	Explosives	Driver Material	Driver Thickness (inches)	Pressure Ramp (kbar)	Ramp Duration (μsec)
13,252	P-40	none	2024 Al	0.500	181-131	2.12
13,253	P-60	none	2024 Al	2.000	150-130	2.20
13,317	P-40	none	Mg	0.500	184-112	2.20
13,318	P-40	none	2024 Al and Lucite	0.500 and 0.500	117-68	2.20
13,330	P-40	none	2024 Al and Lucite	0.375 and 0.375	121-80	1.74

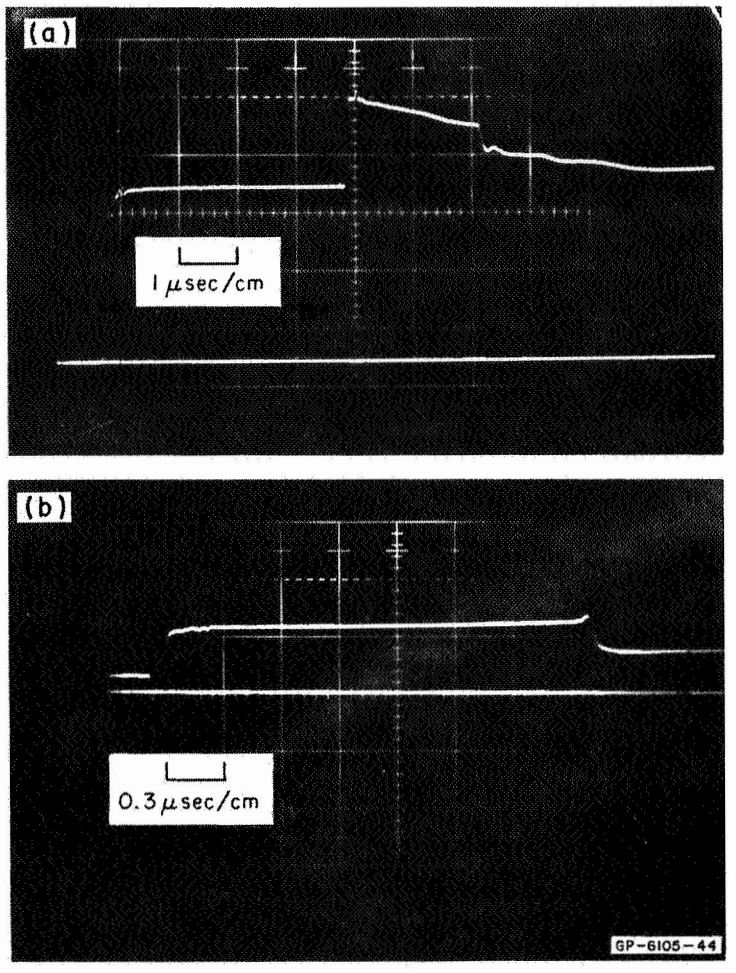

FIG. 12 (a) MANGANIN GAGE RECORD SHOWING PRESSURE RAMP FROM 184 kbar TO 112 kbar; (b) IRON RESISTIVITY RECORD FROM 184 kbar TO 112 kbar

c. Temperature Calibration

A calibration between the temperature and the amplitude and duration of the heating current has been obtained for iron in this project. Figure 14 shows the relative resistance at atmospheric pressure (with respect to room temperature) of iron as a function of temperature. Fig. 15 (a) and Fig. 15 (b) shows the variation of the iron resistance as a function of the heating current duration at current levels of 35 amp and 40 amp, respectively. Figure 16 shows the variation of the iron specimen temperature as a function of the heating current duration at current levels of 40 amp and 35 amp. The curves

TABLE II

Resistivity Data of Iron and Nickel under Shock Loading

Shot No.*	Projectile	Projectile Velocity (mm/μsec)	Pressure (kbar)	Iron Relative Resistance†	Nickel Relative Resistance†
13,477[a]	1/4" thick Al	0.201	23.0	1.16	1.14
13,478[a]	1/4" thick Al	0.380	45.0	1.27	1.27
13,479[a]	1/4" thick Al	0.548	66.0	1.28	1.33
13,480[a]	1/4" thick Al	0.700	86.0	1.61	1.46
13,481[a]	1/4" thick Al	0.878	110.0	1.60	1.50
13,483[a]	1/4" thick Al + 1/8" Brass	0.638	123.5	1.73	1.53
13,484[a]	" " "	0,715	142,5	2.46	1.57
13,482[a]	" " "	0.815	164.0	3.49	----
13,318[b]	---	---	117.0	1.72	----
13,330[b]	---	---	121.0	1.98	----
13,253[b]	---	---	151.2	3.41	----
13,317[b]	---	---	185.0	3.68	----

*Shot numbers with an "a" superscript signify gun shots; those with a "b" signify explosive shots.

†With respect to atmospheric pressure.

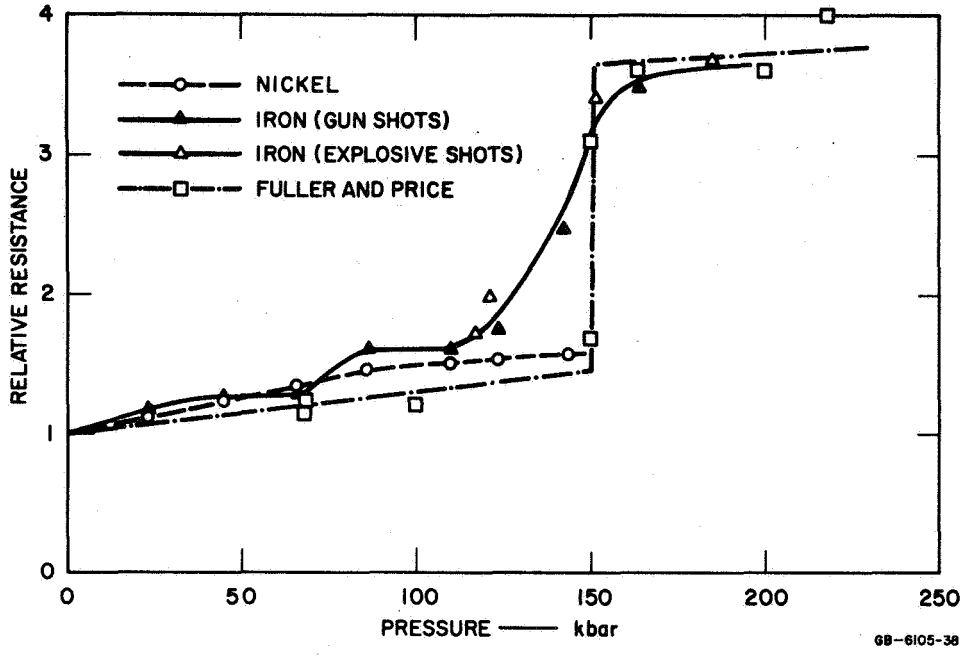

FIG. 13 RELATIVE RESISTANCE OF IRON AND NICKEL AS A FUNCTION OF SHOCK STRESS

shown in Fig. 16 enable one to set the initial temperature of the iron specimen anywhere from room temperature to $\sim 725^{\circ}C$ by adjusting the amplitude and duration of the heating current.

d. Pressure Necessary for Complete Transformation of α- to ϵ-iron

The results of the four double shock experiments are summarized graphically in Fig. 17. Figs. 17 (b), 17 (c), and 17 (d) show the manganin and iron records at pressures of 121, 150, and 181 kbar, respectively. It can be seen from these figures that the transient demagnetization eddy current spike due to the second weaker shock is fairly large at 121 kbar, almost disappears at 150 kbar, and completely vanishes at 181 kbar. The fact that the transient demagnetization eddy durrent spike due to the second shock almost vanishes at 150 kbar indicates that the dynamic $\alpha \rightarrow \epsilon$ polymorphic transformation of iron is almost complete at that pressure. At 181 kbar the dynamic $\alpha \rightarrow \epsilon$ transition of iron is complete, as indicated by the total disappearance of the transient eddy current spike.

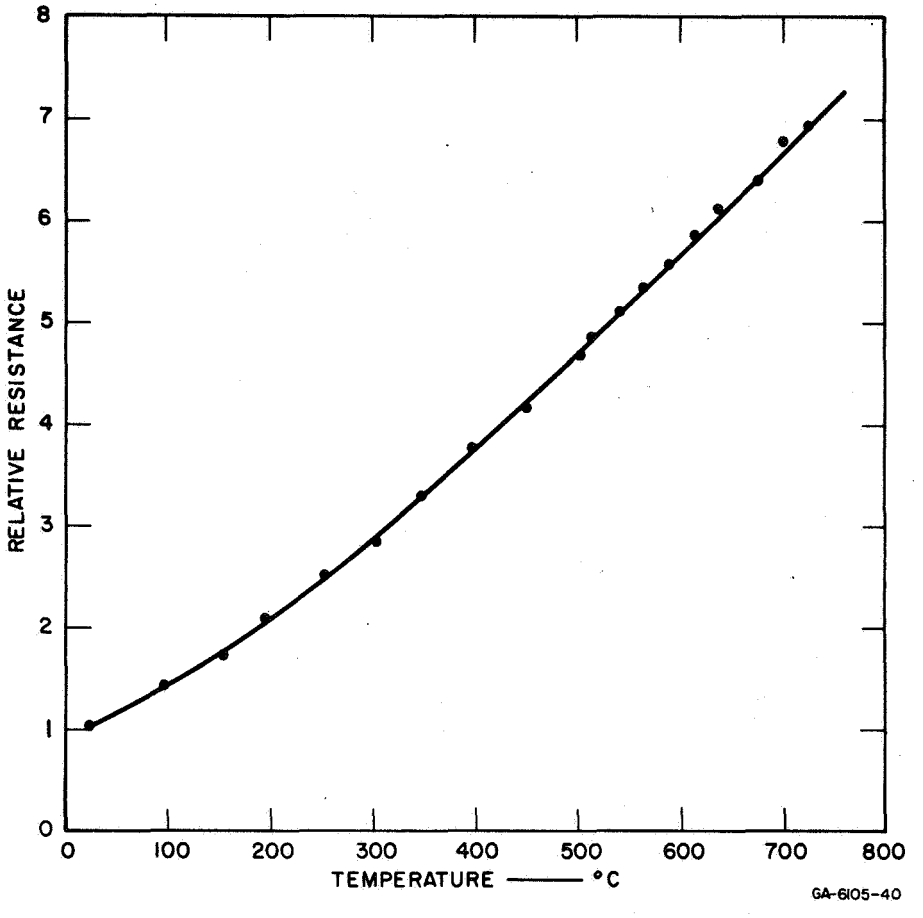

FIG. 14 RELATIVE RESISTANCE OF IRON AS A FUNCTION OF TEMPERATURE

Fig. 17 (a) shows the result of Shot No. 13,345, which was designed to confirm the origin of the second weaker shock by doubling the thickness of the Lucalox backing plate (see Fig. 9) so that the separation in time between the second shock and the main shock should be roughly twice that of the other shots. This is indeed the case, as shown by the figure.

4. Discussion

From the results of the five explosive shock experiments described in Section B-3-a, above, it appears that ϵ-iron, once formed, does not revert automatically to α-iron upon pressure release through the transition pressure for at least 1 μsec. This result is at variance with that implied indirectly by Erkman,[25] namely that ϵ-iron reverts almost instantaneously to α-iron upon pressure release to atmospheric pressure.

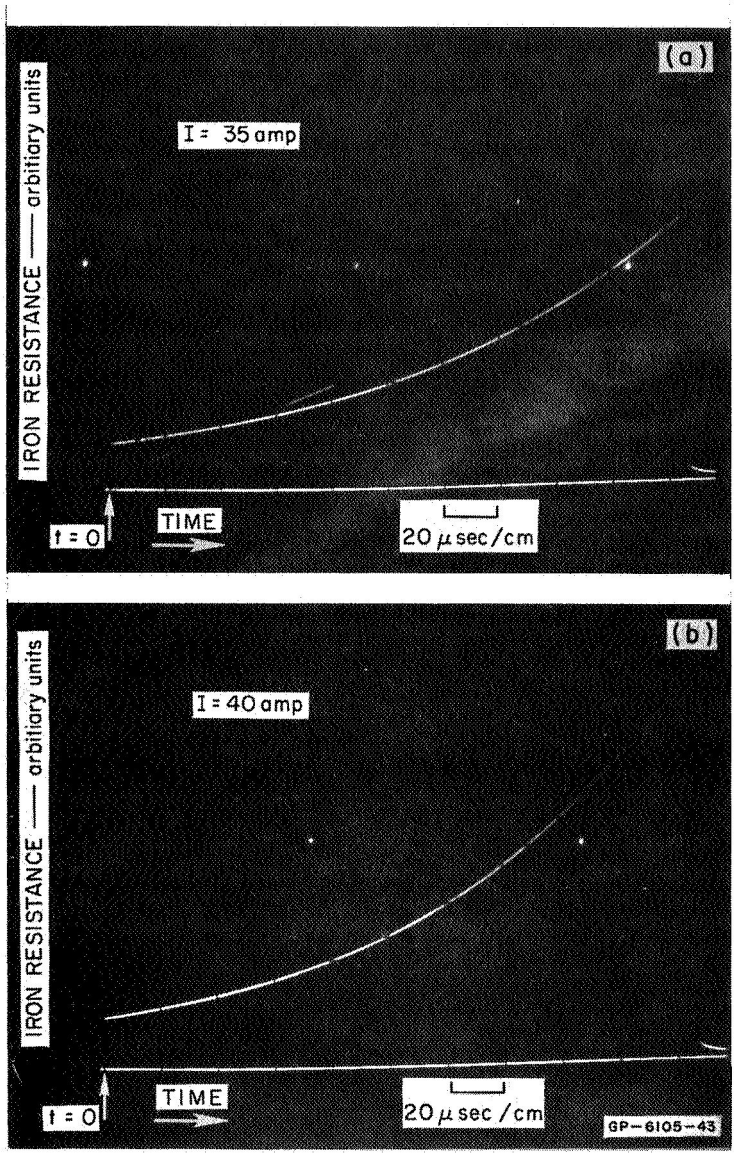

FIG. 15 RELATIVE RESISTANCE OF IRON AS A FUNCTION OF HEATING CURRENT DURATION AT (a) 35 amp AND (b) 40 amp

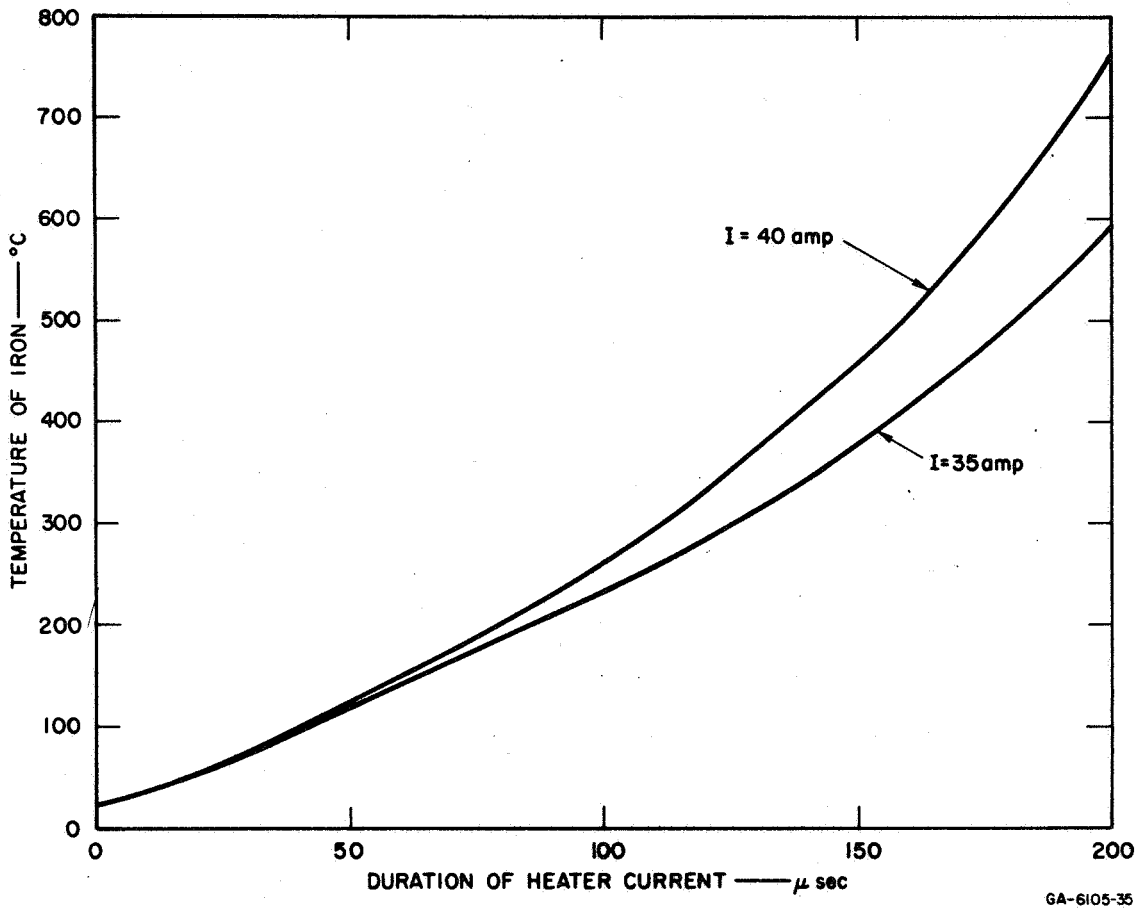

FIG. 16 TEMPERATURE OF IRON SPECIMEN AS A FUNCTION OF HEATING CURRENT DURATION

There are two differences between the present experiment and that of Erkman's. The first one is the rate of pressure release. In the present experiment, the rate of pressure release is ~ 36 kbar/μsec (from 184 kbar to 112 kbar in ~ 2 μsec). The rate is many times greater in Erkman's experiment. However, from considerations of transformation kinetics, the rate of pressure release in the present experiment should favor the reversion from ϵ- to α-iron more than in Erkman's experiment since the rate is smaller. The second difference is the level to which pressure is released. In Erkman's experiment the pressure was released

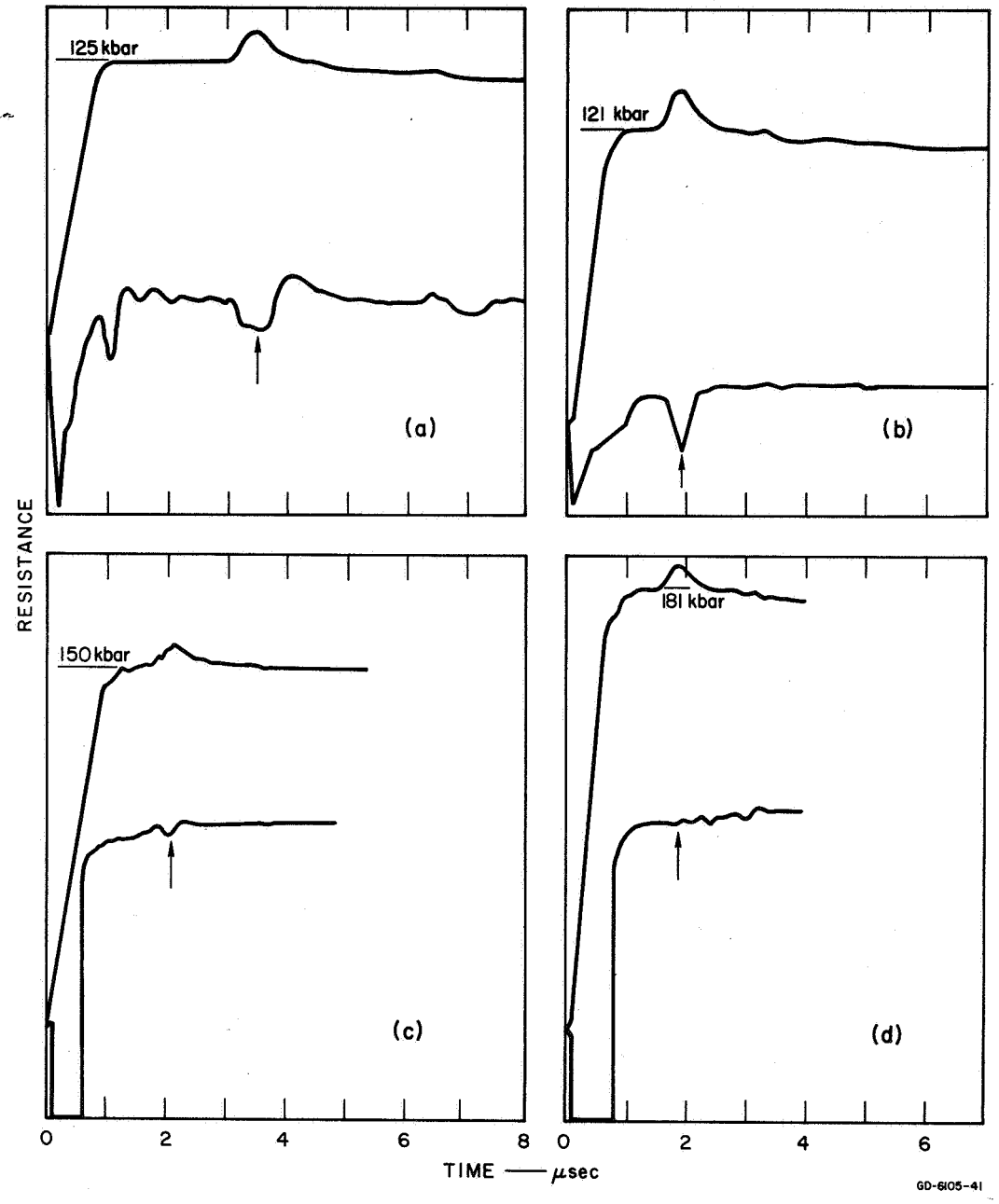

FIG. 17 DOUBLE SHOCK METHOD FOR MONITORING COMPLETENESS OF $\alpha \rightarrow \epsilon$ TRANSITION OF IRON. Upper Trace : Manganin Gage Record; Lower Trace : Iron Resistivity Record

all the way to atmospheric pressure whereas in the present experiment to $\sim$ 112 kbar. It appears therefore that it is the level of pressure release and not the rate that governs the reversion of ϵ- to α-iron.

The persistence of ϵ-iron upon pressure release was observed recently in a static experiment by Mao et al.[28] In this experiment it was observed by X-ray diffraction techniques that ϵ-iron was still detectable to a pressure of 80 kbar when the initial pressure ($\sim$ 180 kbar) was released in steps of $\sim$ 10 kbar. The present dynamic result is consistent with this observation. The only difference is that, whereas the bulk of the ϵ-iron was observed to have transformed back to α-iron by $\sim$ 120 kbar in the static experiment, the present experiment indicates that none of the ϵ-iron has reverted to α-iron during pressure release from 184 kbar to 112 kbar at a rate of $\sim$ 36 kbar/μsec.

The high pressure resistivity data of iron and nickel in Fig. 13 show that iron exhibits a large change in relative resistance in the vicinity of 130 kbar, while no such change occurs for nickel. Fuller and Price[9] interpreted this change in relative resistance as being caused by the $\alpha \rightarrow \gamma$ polymorphic transition of iron, and from their dynamic high pressure resistivity data (see Fig. 13) they placed the $\alpha \rightarrow \gamma$ polymorphic transition of iron at 150 kbar and $\sim 100^{\circ}$C. However, most workers in the field[6,14] currently identify the observed transition as suggested by the dynamic high pressure resistivity data of Fuller and Price with the static $\alpha \rightarrow \epsilon$ transition of iron. The sudden change in relative resistance of iron with pressure observed in the present experiments is therefore interpreted as caused by the $\alpha \rightarrow \epsilon$ polymorphic transformation of iron. Actually, the shocked material may even be a mixture of γ and ϵ phases.

The present high pressure resistivity data of iron were not all measured at precisely the same temperature due to the generation of heat by shock compression (see Section A). However, since Lucalox ceramic was used as the insulation material in the present experiments there is negligible heat flow from the surrounding materials into the iron specimens. This is because the shock impedance of Lucalox ceramic

matches closely that of iron. Hence, the shock temperatures of the Lucalox ceramic and iron are almost identical. The temperature rise in the iron specimens is therefore due entirely to the shock heating of the iron specimen alone. The temperature rise due to shock heating for iron singly shocked to 130 kbar has been estimated to be less than 40°C. Thus, the temperature variation over the present set of high pressure resistivity data of iron is expected to be less than 100°C.

The present dynamic high pressure resistivity data for iron (Fig. 13) show a sudden increase ($\sim 30\%$) in resistance at ~ 80 kbar which is absent in the data of Fuller and Price. This rise in resistance cannot be discounted as an instrumental artifact since nickel was included as a control in each of our experiments, and no abrupt rise in resistance was observed for nickel.

Three mechanisms must be considered as possible causes of this resistance jump. First, as previously suggested by Mitchell and Keeler,[26] the $\alpha \rightarrow \epsilon$ transition might actually start at a lower pressure than has been previously reported. Such an explanation may at first seem likely in the present case because the high pressure resistivity of ϵ-iron is much higher ($\sim 300\%$) than that of α-iron;[18] hence, the partial transformation of α- into ϵ-iron at ~ 80 kbar could account for the observed rise in relative resistance. However, the static resistivity data for iron[18,29] do not show any indication of the onset of such a transformation near 80 kbar. Even if one could associate the rise in resistance of iron with the onset of an $\alpha \rightarrow \epsilon$ transition, one would expect that the resistance of iron would rise continuously, increasing with shock stress between ~ 80 kbar and stress at which the transformation is complete. However, the plateau at ~ 80 kbar would be very difficult to rationalize on this basis unless the $\alpha \rightarrow \epsilon$ transition pressure is strongly orientation dependent.

Second, a shock induced resistivity increase due to creation of lattice defects could account for some rise in the electrical resistivity of iron at ~ 80 kbar. However, the magnitude and abrupt nature of the rise and the subsequent plateau argue against interpreting the entire rise this way. One would expect the most rapid increase in defect

concentration to occur at lower pressures for both iron, and nickel, and in fact the gradual rise in resistivity at lower stresses (Fig. 13) would appear to be caused primarily by shock induced defects. The absence of such an abrupt resistance rise at ~ 80 kbar in the nickel data argues further against this mechanism. It is true that iron differs from nickel in that it is much more easily twinned. In another series of experiments,[30] postshock metallographic examination of iron specimens showed that mechanical twins begin to form in shocked iron below 50 kbar, but terminal resistance measurements showed the magnitude of the resistance increase in heavily twinned samples to be much too small to explain the rise at ~ 80 kbar.

Finally, we are left with the possibility that at least part of the α (b,c.c.) - iron is transformed into a new phase under the influence of the very high shear stresses associated with the shock. This new phase need not even have any field of thermodynamic stability (i.e., it might exist only as a metastable phase). Since the mode of shock compression is plane strain, grains oriented with the $< 100 >$ directions parallel or nearly parallel to the direction of normal shock stress will experience some elastic distortion from cubic to tetragonal structure. Thus, the most likely crystal structure of this dynamic high pressure phase is body-centered tetragonal (b.c.t.), similar to the martensitic α' phase of iron and some of its alloys. If, in fact, the proposed phase is metastable, then for a specimen with randomly oriented grains, only a fraction of the α-iron is expected to undergo this transformation, the transformation ceasing when all the favorably oriented grains have been transformed. Transformation of α-iron into such a metastable phase may not occur at all under a hydrostatic mode of compression.

There is another distinct feature in which the present data for iron differ from those of Fuller and Price. The Fuller and Price data indicate an abrupt high pressure $\alpha \rightarrow \epsilon$ phase transition, whereas the present data indicate that the transformation is a rather gradual one. The presence of some of the proposed b.c.t. phase would be expected to contribute to this graduality, since the b.c.t. $\rightarrow \epsilon$ transition should occur at a different dynamic pressure than the $\alpha \rightarrow \epsilon$ transition. This

gradualness, as suggested by the present data, is consistent with the static high pressure resistivity data of iron obtained by Balchan and Drickamer[29] and supports a simple martensitic model for the $\alpha \rightarrow \epsilon$ transition of iron as proposed recently by Duvall.[31] The present resistivity data indicate that the $\alpha \rightarrow \epsilon$ transition of iron starts at around 120 kbar and completes at around 160 kbar. The results described in Section B-3-d, above, furnish further evidence to support the conclusion that the $\alpha \rightarrow \epsilon$ transition of iron is complete at about 160 kbar.

Although Bancroft et al.[4] detected three stable shocks in iron starting at $\sim$ 130 kbar and interpreted them as caused by the $\alpha \rightarrow \gamma$ polymorphic transition (now identified as $\alpha \rightarrow \epsilon$) in iron, at least two studies[32,33] have suggested that the shock pressure required to produce the characteristic metallographic "matte" appearance associated with the 130-kbar dynamic transition may actually be $\sim$ 155 kbar. One of the objectives of the present project has been to reconcile this discrepancy. The present data indicate that the $\alpha \rightarrow \epsilon$ transformation of iron starts at around 120 kbar. As soon as a critical amount of α-iron has been transformed into ϵ-iron, it is expected that three stable shocks will appear. Thus the observation by Bancroft et al. of three stable shocks in iron at 133 kbar is consistent with the present data. However, the metallographic "matte" pattern characteristic of the $\alpha \rightarrow \epsilon$ transformation of iron will not appear until after the bulk of the α-iron has been transformed into ϵ-iron. Since the present data indicate that the $\alpha \rightarrow \epsilon$ transition is complete at $\sim$ 160 kbar, it is reasonable that the shock pressure required to produce the "matte" pattern should be $\sim$ 155 kbar as observed.

There are several reasons why the present data are more reliable than those of Fuller and Price. First of all, as mentioned in Section A, above, Fuller and Price used a two-pole configuration in the piezoresistive elements of their experiments. With the two-pole configuration the accuracy of measurements can be greatly affected by contact resistance. With the four-pole configuration, as used in the present experiments, the error caused by contact resistance is negligible. Since Fuller and Price

also used a two-pole manganin transducer to monitor the pressure in their experiments, the accuracy of not only the resistance of the iron specimen but also of the pressure reading in manganin might be in error.

Second, instead of using an impedance matching insulating material such as Lucalox ceramic in the construction of their targets, Fuller and Price used a thermosetting resin, which has a very much lower shock impedance than that of iron. The impedance mismatch induces in the iron specimen a transient pressure that is very much higher than that indicated by the manganin transducer. Furthermore, due to the low shock impedance of the thermosetting resin, the resin material experiences very high shock temperatures,[34] and the heat flow into the iron specimen from the surrounding resin is no longer negligible. Since the resistivity of iron is a function of both temperature and pressure, the increase in resistance of the iron specimen due to this extra heating is quite substantial. Moreover, such an increase in resistivity cannot readily be estimated or corrected for. This situation worsens as one goes to higher pressures as the temperature difference between the thermosetting resin and the iron specimen becomes much greater. However, when Lucalox is used as the insulating material, as in the present experiments, no such heating occurs since the shock impedance and hence the shock temperature of the Lucalox ceramic is almost identical to that of iron in the pressure range 0 to 500 kbar. As discussed previously, the shock heating of the iron specimen has been estimated and found to be rather small ($< 100^{\circ}C$).

Third, the shock induced transient demagnetization eddy current spike (see Section A) that appeared at the beginning (i.e., at the arrival of the shock) of every iron resistivity record for all pressures under study had been completely ignored by Fuller and Price. The presence of this eddy current spike, due to its large amplitude, could lead to an erroneous measurement of the iron resistance if not properly taken into account. The present investigators are fully aware of such eddy current spikes and their effects on the measurements of iron resistance have been fully accounted for.

Fourth, since the data of Fuller and Price suggest an abrup $\alpha \rightarrow \epsilon$ transition if iron, they are inconsistent with the static data of Balchan and Drickamer,[29] which indicate the resistance transition is rather gradual and has a spread in pressure of approximately 40 kbar in agreement with the present data. Moreover, an abrupt transition such as that suggested by the data of Fuller and Price cannot reconcile the discrepancy between the Bancroft et al. data on the observation of three stable shocks in iron at 130 kbar and the recent studies on the shock pressures required to produce the metallographic "matte" appearance associated with the $\alpha \rightarrow \epsilon$ dynamic transition of iron.

The dynamic high pressure resistivity data of iron described in Section B-3-b indicate that the $\alpha \rightarrow \epsilon$ transition of iron starts at $\sim$ 120 kbar and completes at $\sim$ 160 kbar. The demagnetization results described in Section B-3-d furnish further evidence that the transition indeed completes at $\sim$ 160 kbar. We believe this is the first time that shock induced transient demagnetization eddy current signals were employed to monitor the completeness of a polymorphic transition of a magnetic material (in this case the $\alpha \rightarrow \epsilon$ transition of iron) as a function of pressure. This technique can be used with equal proficiency in other situations involving polymorphic transitions from a magnetic phase to a nonmagentic phase or vice versa. For example, the same technique can be applied to the $\alpha \longleftrightarrow \gamma$ and $\alpha \longleftrightarrow \epsilon$ polymorphic transitions of iron and iron-nickel alloys at various initial temperatures. Thus, this newly developed technique furnishes a very useful supplementary tool to the resistivity techniques described in Section A above in the studies of dynamic phase transitions of iron and iron-nickel alloys.

The new data on the dynamic response of α-iron under shock loading described in Section I-B-3, above, were presented at the 1968 Gordon Conference on High Pressure Research. From the views expressed at that conference there appeared to be general acceptance by conferees of our new shock wave resistivity data for iron in contrast with those obtained by Fuller and Price. Furthermore, there was general agreement that the dynamic (P,T) phase diagram of iron needs a thorough revision. The discovery of ϵ-iron, once formed, does not automatically revert to

α-iron upon pressure release (experimental pressure release was 36 kbar/μsec for $\geq$ 1 μsec beyond the time of passing through the $\alpha \longleftrightarrow \epsilon$ transition pressure) was received with much interest. Takahashi, one of the conferees, pointed out at the conference that the persistence of ϵ-iron was also observed in his static experiment, but only a small fraction of the specimen remained as ϵ-iron upon pressure release (1 kbar/sec) to $\sim$ 80 kbar. The fact that none of the ϵ-iron was observed to revert to α-iron upon pressure release (36 kbar/μsec), in the present experiments was considered to be a very interesting discovery. The double-shock technique for monitoring the completeness of the dynamic $\alpha \rightarrow \epsilon$ transition of iron (see Section I-B-3d) was also received with much enthusiasm. The presentation of our new data on the dynamic response of α-iron under shock loading appeared to bring considerable satisfaction among conferees that work has finally begun towards clarifying some of the very conflicting data in this field.

C. Conclusions and Recommendations for Further Research

The primary objective of the present program was to study the effects of shock waves on the metallic minerals in iron meteorites, namely iron and iron-nickel alloys. The first part of the program was concerned with the dynamic high temperature and high pressure phase diagrams of iron and iron-nickel alloys. In the course of testing out a new and more efficient method to meet the objective of the program, it was discovered that ϵ-iron, once formed, does not automatically revert to α-iron upon pressure release (at least at a rate $\leq$ 36 kbar/μsec) through the transition pressure for at least 1 μsec. This highly significant discovery is at variance with the data of Erkman,[25] and it is concluded that the reversion of ϵ- to α-iron is governed by the level rather than by the rate of pressure release.

A careful reinvestigation of the dynamic $\alpha \rightarrow \epsilon$ transition of iron using an improved resistivity technique yielded data that are in substantial disagreement with similar data obtained previously by Fuller and Price. However, the present data are consistent with the static resistance data of Balchan and Drickamer. Moreover, they resolve for

the first time the discrepancy between the observation of three stable shocks in iron at 130 kbar by Bancroft et al.[4] and the evidence by two recent investigations[32,33] that the shock pressure required to produce the metallographic "matte" appearance associated with the 130-kbar dynamic transition may be $\sim$ 155 kbar. A critical comparison between the present techniques and those used by Fuller and Price led to the conclusion that the present data are more reliable. It is believed that the present investigation has significantly increased the level of understanding of the $\alpha \rightarrow \epsilon$ dynamic transition of iron.

A resistance heating technique for varying the initial temperature of iron or iron-nickel alloy specimens used as piezoresistive elements in resistivity techniques for studying polymorphic transitions has been successfully developed in this project. This development includes the design and construction of a high current power supply (35 amp at 3.5Kv) with a variable output duration control for use in the resistance heating of iron (or iron-nickel alloys) specimens and a calibration between the temperature and the amplitude and duration of the heating current for iron.

Another technique has been developed during this project utilizing the shock induced transient demagnetization eddy current spike for monitoring the completeness of polymorphic transitions involving a magnetic phase. This newly developed technique furnishes a very useful supplementary tool to the resistivity techniques described in Section A, above, in the studies of dynamic phase transitions if iron and iron-nickel alloys.

It becomes clear from the results of this project that in order to interpret the metallographic features of iron and iron-nickel alloys subjected to shock loading, one must have full understanding of the dynamic phase transitions of these materials. The equilibrium (static) phase diagrams of iron and iron-nickel alloys are useful only to a certain extent since they do not furnish information on the pressures necessary for complete transformations to occur under dynamic situations. Moreover, the experimental high temperature and high pressure phase

diagrams of iron-nickel alloys are largely unexplored, even statically. It is therefore recommended that the dynamic high temperature and high pressure phase diagrams of iron and iron-nickel alloys be investigated, with special emphasis on obtaining the pressures necessary for phase transformations to complete under dynamic situations. The methods to accomplish this objective have been developed during the course of the present program.

II. RECOVERY EXPERIMENTS

A. Introduction

The present study of shock effects in recovered specimens has been conducted in collaboration with Dr. Matthias Comerford of the Smithsonian Institution Astrophysical Observatory. The collaboration has been strictly scientific; no transfer of funds between the two laboratories was involved.

Dr. Comerford provided the samples to be shocked. The shock recovery assemblies were constructed and shock loaded at Stanford Research Institute. Metallographic studies and microhardness measurements were performed both at SRI and at the Smithsonian. Annealing studies were performed at the Smithsonian. Additional annealing experiments and X-ray diffraction studies are currently in progress at the Smithsonian. A journal article, presently in the planning stage, will be jointly authored by SRI and Smithsonian staff members.

B. Shock Loading Experiments

Samples of the Karee Kloof meteorite, the Hoba meteorite, and an iron-2.5% silicon single crystal were selected for the experiments. Karee Kloof is a coarse octahedrite, containing 7.68% nickel. This meteorite was selected because the kamacite plates are relatively undeformed and they are sufficiently wide (~1.7 mm) for detailed X-ray diffraction studies. Hoba is a nickel-rich ataxite, containing 16.2% nickel. The effects of shock waves on nickel-rich ataxite have not previously been studied. Hoba was selected primarily because it is a readily available member of this relatively rare class of meteorites. The iron-2.5% silicon single crystal samples were chosen to provide a single-phase standard to facilitate interpretation of shock effects in the two meteorites.

The meteorite and iron-silicon samples were carefully cut into wafers, approximately 3/4" square by 1/10" thick. Each sample wafer was potted in Wood's metal and sealed in a steel capsule. Each capsule

was placed in a nest of closely fitting concentric rings backed up by an anvil plate. The purpose of the concentric rings and the anvil plate was to protect the sample capsules from the effects of spurious rarefaction waves originating at free surfaces.

Fifteen shock loading experiments were performed, using flyer plate systems developed in the first half of this program (see SRI Quarterly Progress Report 3, pp 10-15) and in earlier research programs. The experimental details are summarized in Table III. Tabulated pressures were computed by the impedance match method, using previously measured values for flyer plate velocity in conjunction with available iron and iron-nickel Hugoniot data. The pressure uncertainties reflect both uncertainties in flyer plate impact veloctiy and uncertainties in the Hugoniots of the sample materials.

The flyer plate systems were designed to transmit a flat topped plane pressure pulse to the specimens. The systems were also designed to provide essentially constant pressures throughout the volume of each specimen.

All of the samples were successfully recovered. The specimens showed no evidence of gross plastic deformation; the nine lowest pressure samples were virtually indistinguishable from control unshocked samples. The absence of gross deformation in these samples is excellent evidence that the shock loading and recovery systems actually performed as intended, viz, to subject the samples to plane shocks of constant intensity throughout the sample volume and relieve the shock pressures via a series of plane rarefactions.

Table III

RECOVERY EXPERIMENTS

Sample No.	Material	Explosive System	Flyer Plate Impact Velocity (km/sec)	Sample Pressure (kbar)
DA-26	Hoba	Plane wave lens, 2.2" diam.; 2.2" diam. x 1" thick Baratol; 1/8" air gap; 1/8" thick 2024 aluminum flyer plate; 3/16" free run	1.84 ± 0.03	235 ± 10
DA-27	Karee Kloof		"	"
DA-28	Iron-2.5% silicon single crystal		"	"
DA-29	Hoba	Plane wave lens, 2.2" diam.; 2.2" diam. x 1/2" thick 9404; 1/8" air gap; 1/8" thick 2024 aluminum flyer plate; 3/8" free run	3.185 ± 0.005	480 ± 15
DA-30	Karee Kloof		"	"
DA-31	Iron-2.5% silicon single crystal		"	"
DA-32	Hoba	Line-initiated mousetrap plane wave, 0.200" E1506D on 0.135" brass flyer at 3.3°	0.41	70 ± 5
DA-33	Karee Kloof		"	"
DA-34	Iron-2.5% silicon		"	"
DA-35	Hoba	Line-initiated mousetrap plane wave, 0.200" E1506D on 0.100" steel flyer plate at 4.35°	0.54	90 ± 5
DA-36	Iron-2.5% silicon single crystal		"	"
DA-37	Karee Kloof		"	"
DA-38	Hoba	Line-initiated Mousetrap plane wave, 0.084" EL 506D on 0.100" steel flyer at 2°	0.25	35 ± 5
DA-39	Iron-2.5% silicon single crystal		"	"
DA-40	Karee Floof		"	"

C. Metallographic Studies

1. Karee Kloof

The kamacite phase of the control specimens indicated very light twinning, on the order of several twins per square millimeter of kamacite. The total area examined, however, was not sufficient to obtain accurate twin density statistics. The twin density appeared to be about a factor of two or three higher in the specimen of Karee Kloof shocked to 35 kbar. However, the twin density in this sample would still be describable as very low, and one may argue that the difference in twin density between control sample and the sample shocked to 35 kbar is statistically insignificant. In the specimen shocked to 70 kbar, the twin density has increased by orders of magnitude over the control. The spacing between adjacent twins has been reduced to 10-20 microns, vs ca 1 mm for the control. The specimen shocked to 90 kbar shows an even higher twin density; the spacing between adjacent plates is in the range 5-10 microns (see Fig. 18). The specimen of Karee Kloof shocked to 235 kbar appears to be very much more densely twinned, and the matrix material between twins is highly distorted. This structure is similar in appearance to microstructures which have been associated with dynamically observed phase transitions in initially iron alloys. This type of microstructure has been variously referred to in the literature as "transformation twinned," "matte" structure, or "ϵ transformation structure". It is more or less accepted at present that this structure results from a shock induced phase transition that reverses on release of pressure. The specimen of Karee Kloof shocked to 480 kbar is similar in microstructure to the 235-kbar specimen.

2. Iron-2.5% Silicon

The control sample appears representative of a good single crystal. No twins are present and neither grain boundaries nor low-angle subboundaries were observed. Metallographic features observed in the shocked samples corresponded roughly to features observable in the kamacite phase of shocked specimens of Karee Kloof. The twin density increased with increasing shock pressure for the 35-, 70-, and 90-kbar experiments. However, the twin density was generally much higher in the

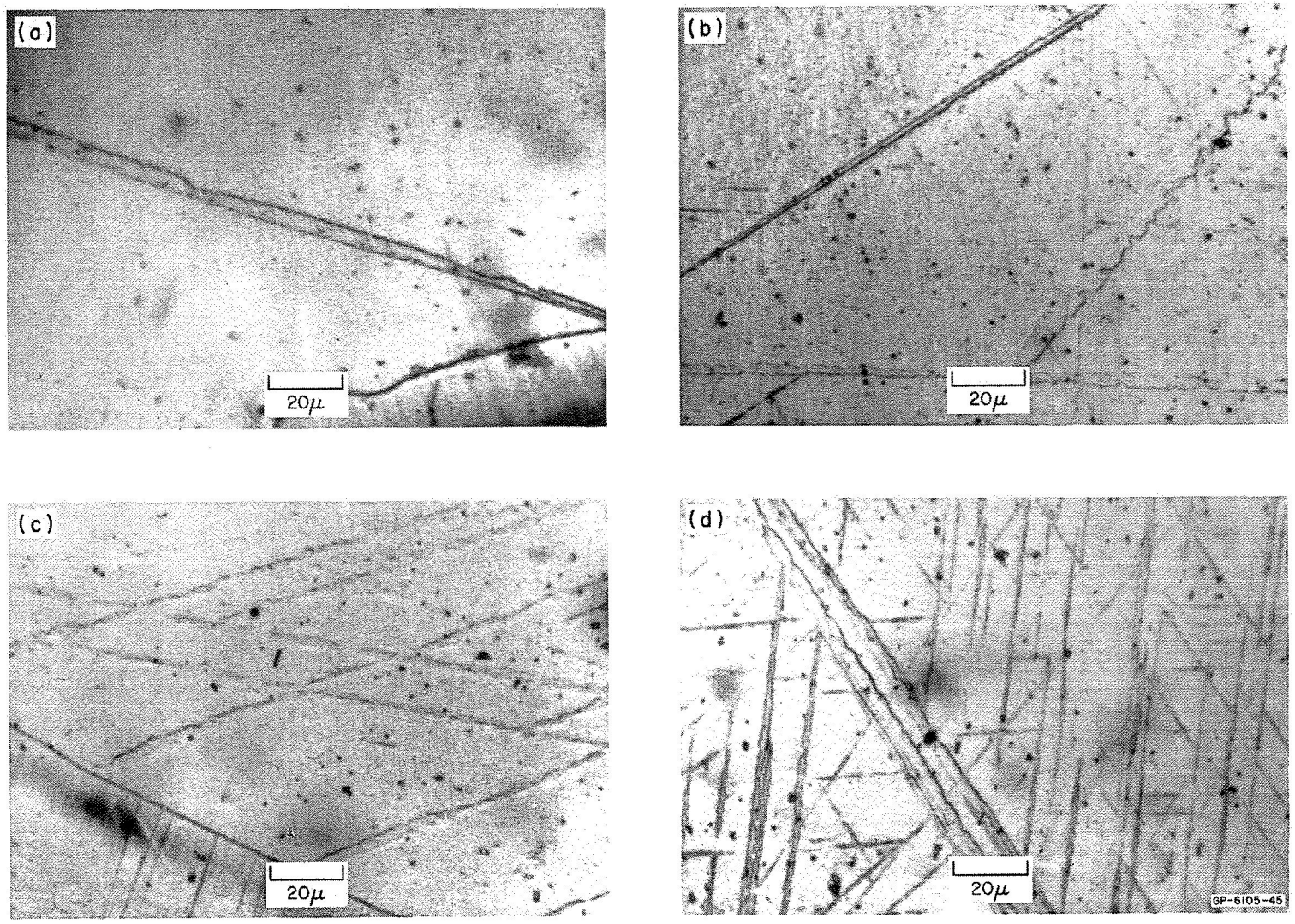

FIG. 18 (a) KAREE KLOOF CONTROL; (b) KAREE KLOOF AFTER 35 kbar SHOCK; (c) KAREE KLOOF AFTER 70 kbar SHOCK; (d) KAREE KLOOF AFTER 90 kbar SHOCK

shocked iron-silicon specimens than in the Karee Kloof kamacite shocked to the same pressure. The twin density in the 35-kbar iron-silicon specimen was similar to the twin density in the 70-kbar Karee Kloof kamacite. The characteristic "matte" or "transformation twinned" microstructure was observed in the specimens shocked to 235 kbar and 480 kbar. The 235 kbar and 480 kbar microstructures are not identical in appearance. Although the major microstructural feature of both structures is heavy banding which could be described as dense twinning, there appears to be less distortion of the matrix material in the 480 kbar specimen (see Fig. 19).

3. Hoba

The results of metallographic examination of control and shocked specimens of Hoba have been most surprising. We have been able to find no significant metallographically observable differences between control and shocked specimens. Dr. Comerford has examined the shocked Hoba specimens and he has also been unable to find unequivocal differences between the shocked and control specimens. One source of difficulty arises from the fact that the kamacite phase in Hoba is distributed primarily in the form of very tiny platelets, averageing only a few microns in width. It is extremely difficult to observe any structural details in these platelets. We have, therefore, concentrated, without success, on looking for shock effects in occasional larger plates of kamacite which are scattered throughout the meteorite specimens.

D. Hardness and Annealing Studies

Hardness changes in the shock loaded specimens were surveyed by Vickers hardness measurements. In this method a pyramidal diamond indenter is used to make an impression on the surface of the specimen. The Vickers hardness number is defined as the load per unit area of surface contact and has the dimensions of kilograms per square millimeter. Vickers hardness numbers are sensitive to applied loads, to an extent that depends on both the work-hardening characteristics of the material and the scale of heterogeneity in the material. For small loads, 1-100 grams, an error arises from the difficulty of accurately measuring the area of the resultant small impressions.

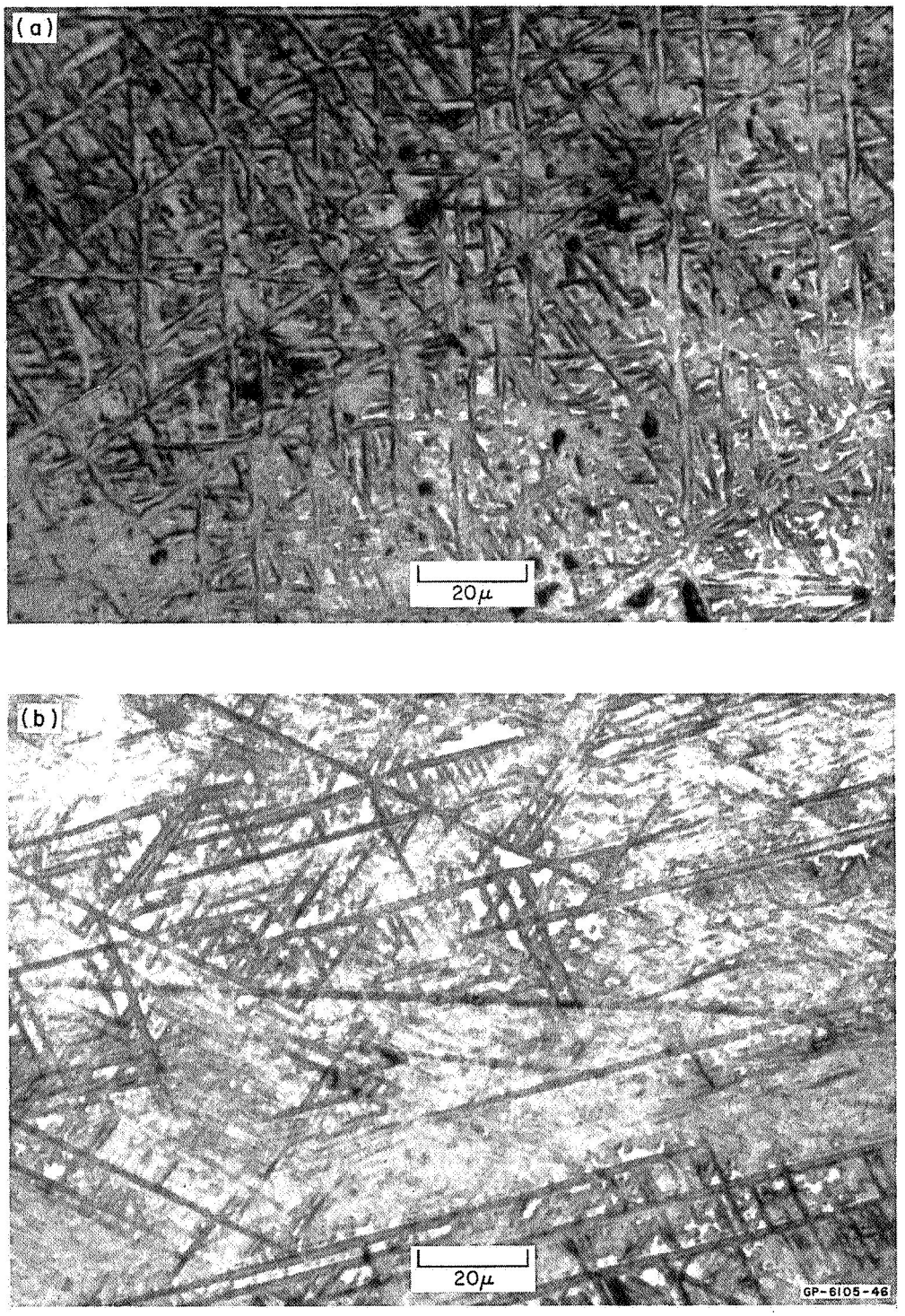

FIG. 19 MATTE STRUCTURE IN SHOCKED Fe–2.5% Si (a) 235 kbar, (b) 480 kbar

The Vickers hardnesses of control specimens of Karee Kloof kamacite and iron-2.5% silicon were in the range 150-180 (100-gram loads). A hardness increase to 200-225 Vickers (100-gram load) was observed for the specimens shocked to 35, 70, and 90 kbar. In this range, 35-90 kbar, the shock induced hardness increase in either kamacite or iron-2.5% silicon did not appear particularly sensitive to shock pressure. A large increase in hardness to Vickers 300-330 was observed in the specimens of Karee Kloof kamacite and iron-2.5% silicon shocked to pressures of 235 and 480 kbar. These results are in agreement with observations made by other workers on shock-loaded iron alloys.[35]

In the case of Hoba, Vickers hardness measurements of both control and shock loaded specimens yielded a wide variation in values, depending on both the applied load and on the region in which a measurement was made. For regions which contained micron-size kamacite platelets, 100 gram-load hardness measurements yielded the same average hardness of 220 Vickers for control sample and for samples shocked to 35, 70, and 90 kbar. With the same load the samples shocked to 235 and to 480 kbar had average hardnesses of 300 and 250 Vickers, respectively. With 500-gram loads, the average hardness of the control specimen was about 220 Vickers; specimens shocked to 35 kbar and to 480 kbar had the same average hardness of about 280 Vickers; specimens shocked to 70 kbar and to 90 kbar had an average hardness of 240 Vickers; and the specimen shocked to 235 kbar had a hardness of about 300 Vickers.

In the control specimen of Hoba there were several kamacite plates of sufficient size to permit 100-gram load hardness measurements. These plates had a hardness of about 175 Vickers, equivalent to the hardness of undeformed kamacite in octahedrites such as Karee Kloof. A similar large kamacite plate in the 235-kbar Hoba specimen had a hardness of 300 Vickers. This latter hardness is equivalent to the hardness of kamacite or iron which has been shocked to pressures of 200 kbar and which shows evidence of the "matte" structure. However, no evidence of the "matte" structure could be found in the kamacite of the 235-kbar Hoba specimen. A single kamacite plate suitable for measurement was found in the 480-kbar Hoba specimen. This plate had a hardness of 200 Vickers, only slightly harder than unshocked kamacite.

The results of annealing experiments on the 235- and 480-kbar specimens of Karee Kloof kamacite, Hoba, and iron-2.5% silicon are presented in Table IV. Metallography indicates that the drastic decrease in hardness of the Karee Kloof and iron-2.5% silicon after the 500° and 600° C treatments is due to recrystallization.

E. Conclusions and Recommendations for Further Research

The dynamic studies of the behavior of iron under shock loading have already provided much evidence relevant to the interpretation of the microstructural and mechanical changes in the recovered shock loaded specimens. Based only on the metallographic and hardness changes, one would be reluctant to suggest that the specimen of Karee Kloof kamacite shocked to 253 kbar had been completely transformed to high pressure phases during passage of the shock. However, on the basis of evidence from the dynamic studies and additional evidence that the transition pressure is lower in 5% nickel-iron than in pure iron, one may argue that the transformation was complete during passage of the shock and that reversion to the low pressure phase occurred during pressure release.

In the 90-kbar experiments with both iron-2.5% silicon and Karee Kloof kamacite we noted a large increase in twin density over the specimens shocked to 70 kbar. It is most interesting that these experiments bracket the pressure region in which a 30% increase of resistivity is observed in the dynamic experiments. Solely on the basis of the dynamic evidence, we have tentatively proposed that a new modification of iron may form in this pressure range. It is possible that the heavily twinned 90-kbar microstructure is associated, at least in part, with the proposed new phase. However, further research, including both dynamic measurements and recovery studies, will be necessary to definitely establish both the existence of the new phase and its relationship to the observed heavy twinning.

The results of both metallographic and microhardness studies of shocked Karee Kloof kamacite and iron-2.5% silicon are in general accord with results obtained by other workers for body-centered cubic iron alloys. However, more experiments will be necessary before we can hope

TABLE IV

Annealing Response of Hardness of Shocked Specimens

Annealing Temperatures (°C)	Vickers Hardness No. (500-gram load)					
	Karee Kloof Kamacite		Hoba		Iron-2.5% Silicon	
	235 kbar	480 kbar	235 kbar	480 kbar	235 kbar	480 kbar
As Shocked	333	297	341	279	328	316
200	340	269	321	270	344	331
300	342	277	303	322	332	382
400	293	250	303	274	302	279
500	227	212	258	273	247	256
600	144	179	229	225	153	172

Note: all samples were annealed for 30 minutes each at the indicated temperature in dry hydrogen.

to establish a pressure scale for shocked meteorites. We are particularly in need of experiments in the 90 to 200-kbar pressure range to investigate the transition between dense twinning and the appearance of the "matte" structure. Our results on the shocked Hoba specimens indicate that shock effects may be difficult to observe in nickel rich ataxites. It is possible that the phase transition, or at least a metallographically observable "matte" structure, may depend critically upon the size of the kamacite plates. One way to investigate this further would be to perform shock experiments on medium, and finest octahedrites.

III. PUBLICATIONS

The following scientific papers were prepared based wholly or in part on the work performed under Contract NASr-49(24):

A. Journal and Symposia Articles

Cowperthwaite, M., and T. J. Ahrens, "Thermodynamics of the Adiabatic Expansion of A Mixture of Two Phases," Am. J. Phys. 35, 951 (1967)

Carter, N. L., C. B. Raleigh, and P. S. De Carli, "Deformation of Olivine in Stony Meteorites", J. Geophys. Res. (in press).

Ahrens, T. J., and J. T. Rosenberg, "Shock Metamorphism: Experiments on Quartz and Plagioclase," Proc. Conf. on Shock Metamorphism of Natural Materials (in press).

De Carli, P. S., "Observations of the Effects of Explosive Shock on Crystalline Solids," Proc. Conf. on Shock Metamorphism of Natural Materials (in press).

Wong, J. Y., R. K. Linde, and P. S. De Carli, "Dynamic Electrical Resistivity of Iron: Evidence for a New High Pressure Phase," Nature (in press).

Wong, J. Y., "Double-Shock Method for Detecting Pressure Limits of Magnetic Phase Transitions," in preparation.

Wong, J. Y., and P. S. De Carli, "Some New Data on the Dynamic Response of α- iron under Shock Loading" (in preparation).

B. Published Abstracts of Oral Presentations

De Carli, P. S., T. J. Ahrens, and J. T. Rosenberg, "Shock Wave Compression of Plagioclase: Maskelynite Formation," Abstracts, 30th Annual Meeting of the Meteoritical Society, October 25-27, 1967.

Petersen, C. F., and T. J. Ahrens, "Shock Temperature in Plagioclase," Abstracts, 30th Annual Meeting of the Meteoritical Society, October 25-27, 1967.

De Carli, P. S., and R. K. Linde, "Geophysical and Geochemical Implications of Shock Wave Data on Oxide Rocks and Minerals," Trans. Am. Geophys. Union 49, 310 (1968).

Publications (continued)

Ahrens, T. J., and C. F. Petersen, "Shock Compression and Adiabatic Release of Feldspars," Trans. Am. Geophys. Union 49, 310 (1968).

C. Oral Presentations

De Carli, P. S., "Shock Wave Compression of Plagioclase: Maskelynite Formation," presented at the 30th Annual Meeting of the Meteoritical Society, October 25-27, 1967.

Petersen, C. F., "Shock Temperature in Plagioclase," presented at the 30th Annual Meeting of the Meteoritical Society, October 25-27, 1967.

De Carli, P. S., "Geophysical and Geochemical Implications of Shock Wave Data on Oxide Rocks and Minerals," presented at the 49th Annual Meeting of the American Geophysical Union, April 8-11, 1968.

Ahrens, T. J., "Shock Compression and Adiabatic Release of Feldspars," presented at the 49th Annual Meeting of the American Geophysical Union, April 8-11, 1968.

Wong, J. Y., "New Data on the Shock Wave Phase Transformation of Iron," presented at the Gordon Conference on High Pressure Research, June 17-21, 1968.

De Carli, P. S., "Some New Shock Wave Results," presented at the Gordon Conference on High Pressure Research, June 17-22, 1968.

REFERENCES

1. Howe, H. M., Metallography of Steel and Cast Iron, McGraw-Hill, New York, 1916.

2. Harnecker, K., and E. Rassow, Zeitschrift für Metallkunde 16, 312 (1924)..

3. Rinehart, J. S., and J. Pearson, Explosive Working of Metals, Macmillan, New York, 1963.

4. Brancroft, D., E. L. Peterson, and S. Minshall, J. Appl. Phys. 27, 291 (1956).

5. Curran, D. R., and P. S. De Carli, Technical Report 014-58, Stanford Research Institute, 1958 (unpublished).

6. Jamieson, J. C., and A. W. Lawson, J. Appl. Phys. 33, 776 (1962).

7. Kaufman, L., Discussion of Paper by C. M. Fowler, F. S. Minshall, and E. G. Znkas, in Response of Metals to High Vlocity Deformation, P. G. Shewmon and V. F. Zackay, eds., Interscience, New York, 1961, pp. 300-306.

8. Curran, D. R., S. Katz, J. J. Kelly, and M. W. Nicholson, Trans. AIME 215, 151 (1959).

9. Fuller, P. J. A., and J. H. Price, Nature 193, 262 (1962).

10. Johnson, P. C., B. A. Stein, and R. S. Davis, J. Appl. Phys. 33, 557 (1962).

11. Tardif, H. P., F. Claisse, and P. Chollet, "Some Observations on Explosively Loaded Iron and Mild Steel," Response of Metals to High Velocity Deformation, P. G. Shewmon and V. F. Zackay, eds., Interscience, New York, 1961, pp. 389-407.

12. Dieter, G. E., "Metallurgical Effects of High-Intensity Shock Waves in Metals," Response of Metals to High Velocity Deformation, P. G. Shewmon and V. F. Zackay, eds., Interscience, New York, 1961, pp. 409-444.

13. Zukas, E. G., and C. M. Fowler, "The Behavior of Iron and Steel Under Impulsive Loading," Response of Metals to High Velocity Deformation, P. G. Shewmon and V. F. Zackay, eds., Interscience, New York, 1961, pp. 343-368.

14. Takahaski, T., and W. A. Bassett, Science 145, 483 (1964).

15. Nivikov, S. A., I. I. Divnov, and A. G. Ivanov, Fiz. Metal. Metalloved. 20, 133 (1965).

16. Nivikov, S. A., I. I. Divnov, and A. G. Ivanov, Fiz. Metal. Metalloved. 21, 252 (1966).

17. Doran, D. G.,and R. K. Linde, "Shock Effects in Solids," Solid State Physics, 19, F. Seitz and D. Turnbull, eds., Academic Press Inc., New York (1966).

18. Bundy, F. P., J. Appl. Phys. 36, 616 (1965).

19. Perez-Albuerne, E. A., F. K. Forsgren, and H. G. Drickamer, Rev. Sci. Instr. 35, 29 (1964).

20. Kaufman, L., E. V. Clougherty, and R. J. Weiss, Acta Met. 11, 323 (1963).

21. Bernstein, D., and D. D. Keough, J. Appl. Phys. 35, 1471 (1964).

22. Florence, A. L., and T. J. Ahrens, "Interaction of Projectiles and Composite Armor," Final Report, Stanford Research Institute, Contract DA-04-200-AMC-138(X), January 31, 1967.

23. McQueen, R. G., and S. P. Marsh, J. Appl. Phys. 31, 1253 (1960).

24. Goranson, R. W., et al., J. Appl. Phys. 26, 1472 (1955).

25. Erkman, J. O., Appl. Phys. 32, 949 (1961).

26. Mitchell, A. C., and R. N. Keeler, Bull, Am. Phys. Soc. 12, 1128 (1967).

27. Royce, E. B., J. Appl. Phys. 37, 4066 (1966).

28. Mau, H., W. A. Bassett, and T. Takahashi, J. Appl. Phys. 38, 272 (1967).

29. Balchan, A. S., and H. G. Drickamer, Rev. Sci. Instr. 32, 308 (1961).

30. De Carli, P. S., unpublished work.

31. Duvall, G. E., private communication.

32. Curran, D. R., Final Report PGU-2912, Stanford Research Institute (1963).

33. Katz, S., D. G. Doran, and D. R. Curran, J. Appl. Phys. 30, 568, (1959).

34. Keough, D. D., Final Report PGU-3713, Stanford Research Institute (1964).

35. Dieter, G. E., "Hardening Effects of Shock Waves," in Strengthening Mechanisms in Solids, American Society for Metals, Metal Park, Ohio, 1962.

STANFORD RESEARCH INSTITUTE

Main Offices and Laboratories

333 Ravenswood Avenue
Menlo Park, California 94025
(415) 326-6200
Cable: STANRES, Menlo Park
TWX: 910-373-1246

Regional Offices and Laboratories

Southern California Laboratories
820 Mission Street
South Pasadena, California 91030
(213) 799-9501 • 682-3901
TWX: 910-588-3280

SRI-Washington
1611 North Kent Street, Rosslyn Plaza
Arlington, Virginia 22209
(703) 524-2053
Cable: STANRES, Washington, D.C.
TWX: 710-955-1137

SRI-New York
200 E. 42nd Street
New York, New York 10017
(212) 661-5313

SRI-Huntsville
Missile Defense Analysis Office
4810 Bradford Blvd., N.W.
Huntsville, Alabama 35805
(205) 837-3050
TWX: 810-726-2112

SRI-Chicago
10 South Riverside Plaza
Chicago, Illinois 60606
(312) 236-6750

SRI-Europe
Pelikanstrasse 37
8001, Zurich, Switzerland
27 73 27 or 27 81 21
Cable: STANRES, Zurich

SRI-Scandinavia
Skeppargatan 26
S-114 52 Stockholm, Sweden
60 02 26; 60 03 96; 60 04 75

SRI-Japan
Edobashi Building, 8th Floor
1-6, Nihonbashi Edobashi
Chuo-ku, Tokyo
Tokyo 271-7108
Cable: STANRESEARCH, Tokyo

SRI-Southeast Asia
Bangkok Bank Building
182 Sukhumvit Road
Bangkok, Thailand
Bangkok 910-181
Cable: STANRES, Bangkok

Representatives

France
Roger Godino
94, Boulevard du Montparnasse
75 Paris 14e, France
633 37 30

Italy
Lorenzo L. Franceschini
Via Macedonio Melloni 49
20129, Milan, Italy
72 32 46

Portugal
J. Gasparinho Correia
Avenida Joao XXI, 22-3° Esq.
Lisbon, Portugal
72 64 87

April 1968